

# Spatial Screening of Climate-related Natural Hazards in Senegal<sup>1</sup>

## I Introduction

Senegal is a country located in West Africa, bordered by Mauritania to the north, Mali to the east, Guinea to the southeast, and Guinea-Bissau to the south. On the west it is bordered by the Atlantic Ocean, with a coastline of about 700 km. The country has a varied landscape, including the Sahel region in the north, which is a semi-arid area characterized by sparse vegetation and dry conditions. To the south, there is a more fertile area known as the Sudanian zone, which is characterized by grasslands, woodlands, and savannas (*Figure 1*). Important hydrological features include the Senegal river (perennial) on the northern border, discharging partially in the Lac de Guéris and on the Atlantic coast; the Gambia river (perennial) crossing the South until the Gambia border; the Casamance rivers (perennial) near the south-west border; and the Saloum river (non-perennial), flowing into a large delta before the Atlantic Ocean. The site comprises brackish channels encompassing over 200 islands and islets, covered in mangrove forest [[Africa Groundwater Atlas 2019](#)].

*Figure 1: Natural map of Senegal with main surface water bodies*



<sup>1</sup> Prepared by A. H. Essenfelder and M. Amadio [mamadio@worldbank.org]

Senegal is located in the intertropical zone with two major climatic domains (*Figure 2*). The northern part of Senegal has a warm desert climate, the central part has a warm steppe climate and the southern part a tropical Savannah climate. Two distinct seasons characterize Senegal's climate: a dry season from roughly October to May and a rainy season from June to September. While the arid zones receive a rainfall total under 300 mm/year per year, the forested south receives an average of 1,200 mm/year. Rainfall is highly variable

both on the interannual and inter-decadal timescales. The seasonal variability is affected by the migration of the intertropical convergence zone (ITCZ), which is the front of low pressure at which hot, dry continental air meets moist oceanic air and produces heavy rainfall. The average annual temperature for Senegal was 27.8°C for the period 1960-1990, with monthly averages in the hottest seasons of up to 35°C [[WB CCKP, 2022](#)]. The coastal region is generally cooler than the inland areas, thanks to the ocean breeze. The landscape of Senegal is largely dominated by woody savannah and herbaceous vegetation. Senegal is a predominantly rural country: agriculture is the main economic activity in Senegal, accounting for around 16% of the country's GDP. Crops grown include groundnuts, cotton, millet, sorghum, and rice. Yet cropland covers only about 6% of the country territory [[EEA 2020](#)]. Fishing is also an important industry, with Senegal's coastline being rich in fish stocks. Mining is a growing sector in the country, with Senegal being one of the largest producers of phosphate in the world [[The World Factbook, 2022](#)].

Senegal is exposed to various natural hazards, including floods, droughts, and coastal erosion [[GFDRR](#)]. The count of extreme events as recorded in EM-DAT [[2022](#)], in Senegal between 1965 and 2021 reports 35 major disasters. *Figure 3* shows the number of disasters by regions (ADM level 1).

**Floods** are the most frequent natural hazard in Senegal, occurring on average every two years over the past 30 years, particularly during or following the rainy season (July to October).

**Droughts** are also a significant hazard in Senegal, particularly in the north of the country, which is part of the Sahel region. In the last 50 years, the country has experienced nine important droughts. While less frequent than floods, drought spell have a long duration and aftermath, posing serious threats to food security and livelihoods (famine) across the whole country. According to the World Food Program [[2022](#)], more than 750,000 people in Senegal are currently facing food insecurity as a result of drought and other factors.

**Coastal flooding and erosion** affect the low-lying areas along the Atlantic coast. Rising sea levels and changing weather patterns are contributing to the erosion of beaches and the loss of land, which can have significant impacts on the population and the economy. According to UNDP Senegal Climate Risk

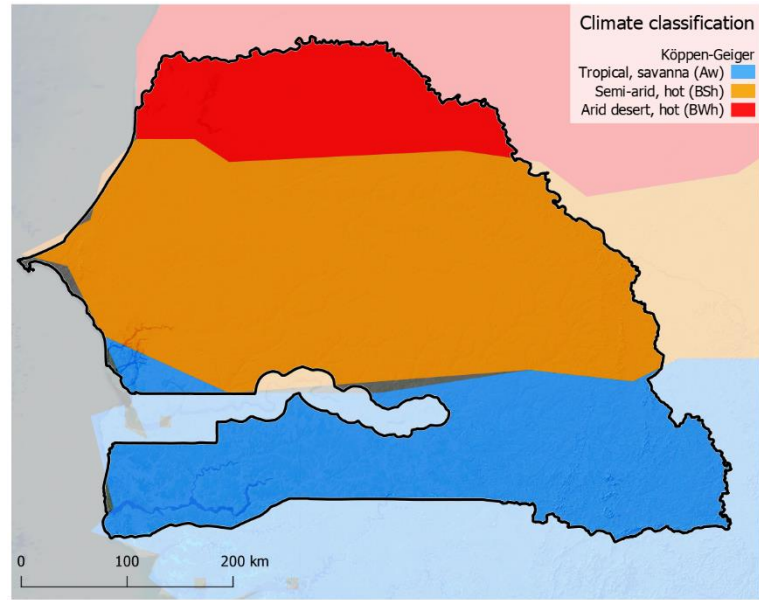
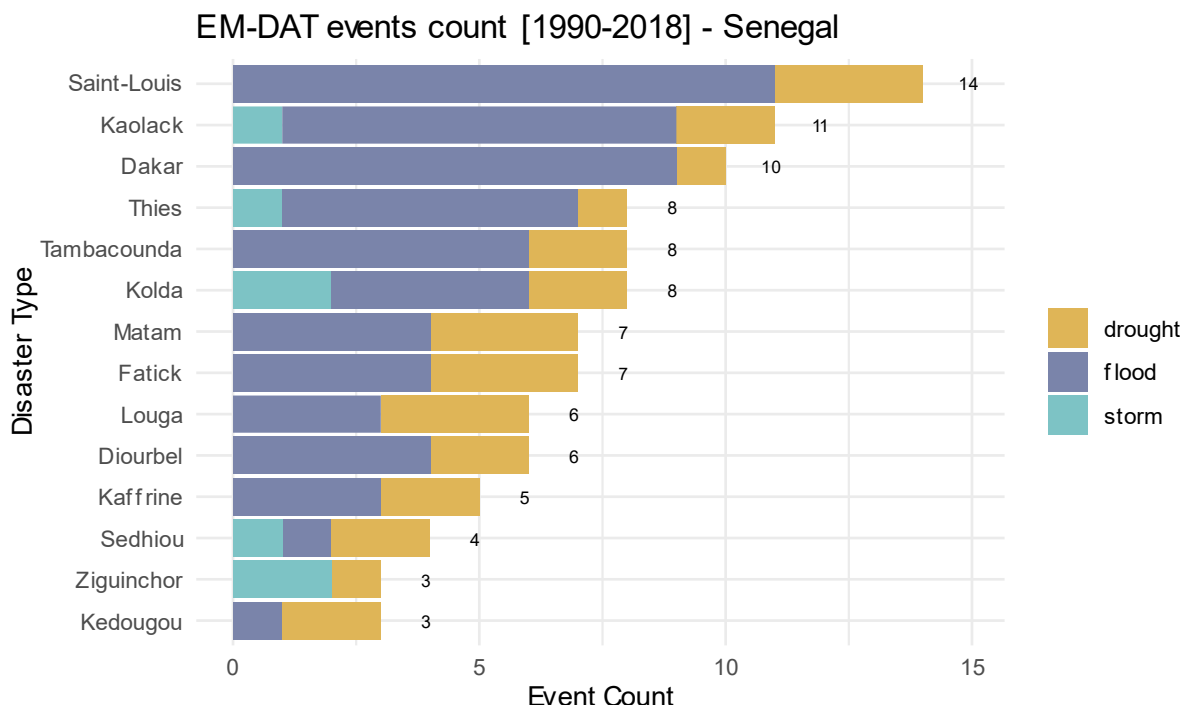


*Figure 2: Köppen-Geiger climate classification of Senegal*

Profile, more than 150,000 people in Senegal are at risk of displacement due to coastal erosion [[UNDP 2017](#)].

Senegal is also at risk of **extreme heat stress**, as it experiences high temperatures and humidity levels throughout the year, particularly in the central and northern regions. This can affect human health, agriculture, livestock, and the economy. The risk of heat stress is further increased by factors such as poor air quality, lack of access to clean drinking water, and limited healthcare resources.

*Figure 3: disaster events reported by EM-DAT between 1990 and 2018 for Senegal at ADM1 level. Note that the same event could involve more than unit.*

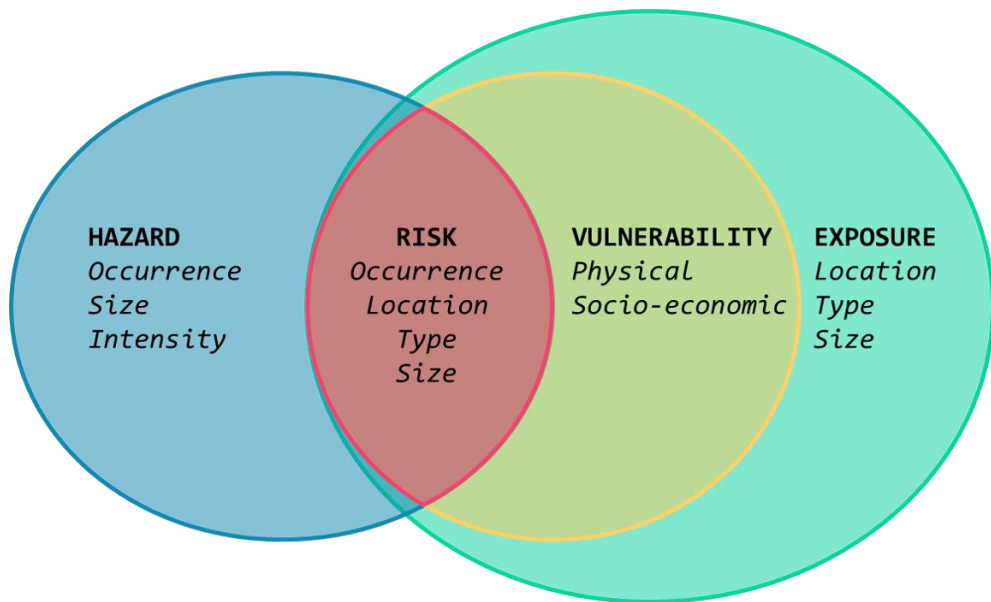


These climate risks are however unevenly distributed across the country and depend on the probability and intensity with which a hazard occurs, the exposure to peoples and their assets, and their vulnerability to various hazard. In general, poorer households are least resilient to climate affects because they tend to reside in more disadvantaged and hazard-prone areas, have lower access to critical services like health, education and early warning systems, and their assets [[Hallegatte et al. 2018](#)]. This report provides an overview of exposure and risks associated with flooding (riverine and coastal), droughts, heat stress and air pollution across Senegal, with a future outlook about the expected variability for these hazards.

## 2 Definitions and Methodology

### 2.1 Disaster Risk

Disaster risk is the probability of a negative impact caused by a natural hazard. The United Nations Office for Disaster Risk Reduction (UNDRR) defines natural hazard as potential events or trends that may cause loss of life, injury, or other health impacts, and damage and losses to property, infrastructure, livelihoods, service provision, ecosystems and environmental resources [UNDRR]. Exposure characterizes the location of people and their assets which may be threatened by natural hazards [UNDRR]. While people (and their assets) may get exposed, they may not be adversely impacted by hazards if they are not vulnerable [UNDRR]. Together, hazard (*H*), exposure (*E*), and vulnerability (*V*) drive disaster risk (*R*). More details about the methodology are available online [[GFDRR/CCDR-tools](#)].



### 2.2 Hazard

Natural events (including extreme events and long-term phenomena) are only termed hazards when they have the potential to harm people or cause property damage, social and economic disruption. The location of natural hazards primarily depends on geography, environmental conditions (such as presence of water bodies, slopes, vegetation) and natural processes, including the influence of weather systems and tectonic movements. Anthropic processes such as urbanization, environmental degradation and climate change can also influence the location, occurrence frequency and intensity of natural hazards. These are known as risk drivers.

Hazards intensity can be modelled following two different approaches:

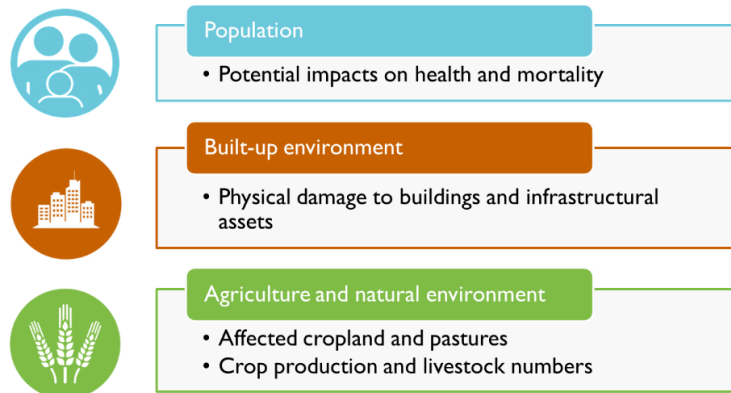
- a. **Deterministic**, in the form of an individual geodata layer measuring the mean, median or maximum intensity of a hazard aggregating historical data and modeling. This is the case for droughts and air pollution.
- b. **Probabilistic**, in the form of multiple geodata layers, each representing a range of hazard physical intensities (e.g. water depth [metres], wind speed [km/h]) corresponding to a specific occurrence frequency, measured as Return Period (RP), in years. This is the case for river and coastal floods.

Hazard models carry limitations related to their applicability, as their quality depends on scale, resolution, model, and input data. As a rule of thumb, their fitness for application in the context of a risk screening or assessment exercise depends on the scale of the risk analysis, i.e. locally-sourced models are expected to be best fitted for local scale assessment (e.g. city level), while global models are best suited for national or sub-national estimates. In the context of developing countries, however, a global model is often the only available source. In such cases, the application of the global model must be taken with caution and correctly interpreted acknowledging the limitations.

## 2.3 Exposure

Exposure describes the location of people and assets that are prone to suffer an impact from natural hazards. We consider three exposure categories used as main indicators of risk, listed in *figure 6*.

*Figure 6: exposure categories considered in the analysis and related impact types*



Each indicator is quantified by a specific metric: *population* is described in terms of total count per area and as share of total population within an administrative unit, while *built-up* and *agricultural land* environment are measured in terms of area (hectares) and share over total land area within the administrative unit.

## 2.4 Vulnerability

Vulnerability is determined by physical, social, economic, and environmental factors or processes, which increase the susceptibility of an individual, their assets or a community, to hazards [[UNDRR](#)]. Two main components of vulnerability are typically accounted for in this note:

**Impact models**, draw the relationship between the intensity of hazard and the predisposition of damage suffered by specific exposed categories into actual impact; e.g., a flood depth of 0.5m is expected to cause a low degree of impact in terms of population mortality, while a 3m flood would cause severe impact. Impact models can be quantitative, providing an absolute or relative estimate of the damage (i.e., in terms of USD or % of total value); or qualitative, classifying the impact in nominal categories.

**Socio-economic conditions:** Describe the differential susceptibility of exposed categories to suffer damage, i.e., areas under poverty conditions and high dependency rate are more likely to suffer damage compared to wealthy communities, under the same hazard event. These are measured using spatial indices based on demographics (sex, age composition, dependency rate) and socioeconomic statistics (wealth, GDP and average salary, among others), and are semi-quantitative metrics (index score; ranking).

Not all exposure categories are affected in the same way by physical hazards - some hazards are more relevant for one category than another. The impact model needs to be aligned with the hazard

intensity metric, with the exposure category, and with the socio-economic conditions to which they are applied to. For this reason, the availability of such models dictates the possible combinations of hazard and exposure categories. As no country- or sub-country-specific impact functions are available for Senegal, we rely on the utilization of global- or regional-level impact functions. *Table 1* identifies which combinations are sustained by currently available impact models, and which can only be classified in terms of exposure to hazard classes, defined using hazard intensity thresholds based on literature studies. More details about the impact models for each combination are given in Annex 3.

*Table 1: Available Hazard, Exposure, and Vulnerability components for Senegal*

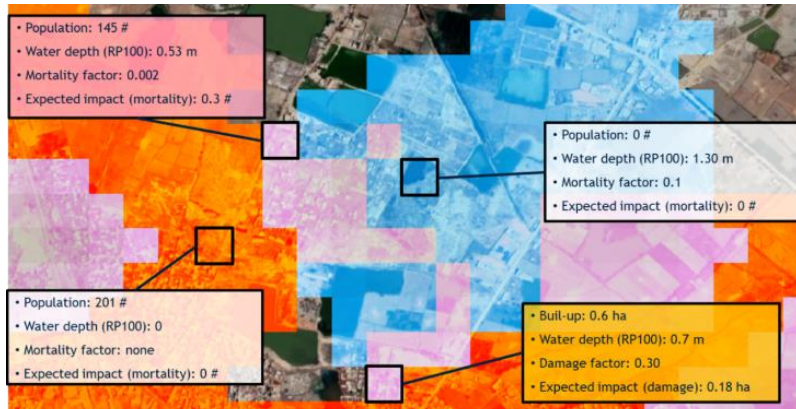
Hazard types	Exposure categories		
	Population (Mortality)	Built-up assets (Physical damage)	Agricultural land (Production losses)
River and Coastal floods <i>Probabilistic</i> [Water extent and depth]	Impact model	Impact model	Exposure by hazard classes
Landslides <i>Deterministic</i> [Landslide hazard index]	Exposure by hazard classes	Exposure by hazard classes	
Agricultural drought <i>Deterministic</i> [Agricultural Stress Index]			Exposure by hazard classes
Heat stress <i>Probabilistic</i> [Heat index]	Exposure by hazard classes		
Air pollution <i>Deterministic</i> [PM2.5 concentration]	Exposure by hazard classes		

The socio-economic component is added after the baseline risk calculation to highlight where the risk is expected to translate into most severe impacts (see chapter 2.6).

## 2.5 Baseline risk - Expected Annual Exposure and Impact

*Baseline risk* refers to an estimate related to the historical period to which the data refer, as opposed to future risk (*climate outlook*). Baseline risk is calculated by combining geospatial hazard and exposure data. Locations with no hazard or no exposure are excluded from calculations. The unit of analysis is set to a resolution that matches that of the selected exposure layers. The impact model translates the physical intensity unit of a specific hazard into a damage factor (0 to 1), which is then multiplied by the exposure layer to obtain the impacted share over the total exposed value (*figure 7*).

*Figure 7: example of hazard, exposure and vulnerability components combined in GIS environment. The flood hazard layer (blue) describing water extent and depth (m) overlays the exposure layer (orange) which describes population count or built-up area. Where they match, there is an impact (pink) which is calculated as the product of the total exposure and the damage factor, driven by the impact model: depth-mortality function in the case of population (top-left box), depth-damage function in the case of built-up (bottom-right box).*



When probabilistic hazard scenarios are available, the expected annual impact (EAI) is calculated by multiplying the impact from each event scenario with its exceedance probability ( $1/RP_i - 1/RP_{i+1}$ ), and then summing up to one value; else, if no impact function is available, the expected annual exposure (EAE) is calculated for a selected hazard threshold. The exceedance frequency curve (*figure 8*) highlights the relationship between the return period of each hazard and the estimated impact. The area below the curve represents the total annual damage considering all scenario probabilities.

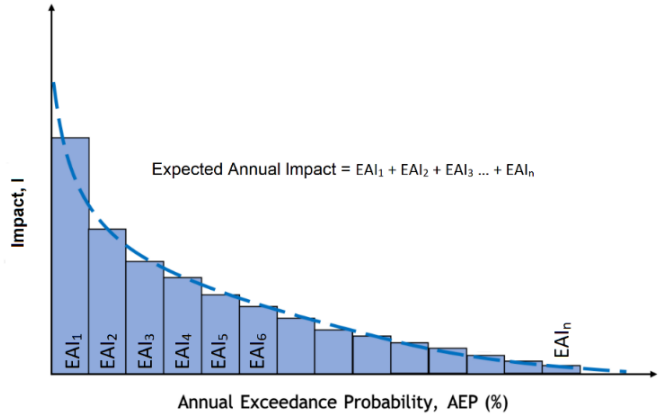
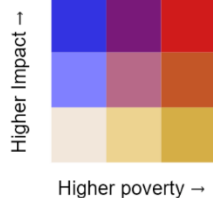


*Figure 8: Computation of Annual Expected Impact of natural hazards in geospatial analytics*

## 2.6 Risk and Poverty

The distributional impact of climate risks can be examined by overlaying risk maps (EAI or EAE) with poverty maps [[Bangalore et al. 2019](#)]. The combination is displayed using bivariate maps that show the locations where risk is most likely to translate into most severe impacts on the poorest and vulnerable households.



The estimate of poverty distribution is usually done measuring either the income distribution (of the household's dwellers), or expenditure (average monthly expenditure of the household). However, due to the difficulties in obtaining reliable income/consumption data in low- and middle-income countries, alternative ways to build the wealth index are often the best available approximation of relative socio-economic status. The presence of physical assets in the household can be used to construct a wealth index [[Filmer and Pritchett 2001](#)]. Relative wealth indices are an equally valid, but distinct measure of household socio-economic status from income and consumption measures [[Poirier et al. 2019](#)]. Context-specific factors such as country development level may affect the concordance of health and educational outcomes with wealth indices and urban–rural disparities can be more pronounced using wealth indices compared to income or consumption.

AI-based indices such as the **Relative Wealth Index (RWI)** [[Chi et al. 2022](#)] are appealing due to the immediate and cost-effective estimates they can provide. The RWI is an index estimated by a machine learning model for 135 low and middle-income countries to provide micro-estimates (projections) of wealth and poverty at fine-grained 2.4 km resolution tiles. The model is trained on vast and heterogeneous datasets from satellites, mobile phone networks, topographic maps, as well as connectivity data from Facebook. The approach for creating the RWI map overcomes essential limitations of the traditional surveys, such as fine-grained coverage, and timely and cost-efficient data, while extending to countries where DHS does not operate. However, the application of RWI index to a real-world scenario is sensitive to the socioeconomic particularities of the country, leading to likely different estimates from the ones obtained by a traditional survey approach.

### 3 Climate outlook

The forward-looking analysis uses future climate projections to explore how environmental risks could develop spatially across the West Africa region. The long-term averages of climate indices (observed or simulated) serve as the baseline conditions, against which the effects of climate change are measured for future scenarios. Changes in projected climate indices against this baseline (anomalies) and used to estimate changes in natural hazard frequency and intensity. Given that specific unit of measurement varies across climate indices, all changes against the baseline are expressed in terms of Standard Deviation (SD) of the anomaly compared to historical variability [E3CI, 2020]. Data from climate models released under the IPCC Sixth Assessment Report (AR) framework [[IPCC 2021a](#)] are used to establish estimates of baseline and future projected climate anomalies. ARs are supported by coordinated climate modeling efforts referred to as Coupled Model Intercomparison Projects (CMIP). The analysis relies on CMIP6 data for modeling into the future, and takes into account four climate change scenarios, referred to as Shared Socioeconomic Pathways (SSPs) in CMIP6. These pathways cover the range of possible future scenarios of anthropogenic drivers of climate change by accounting for various future greenhouse gas emission trajectories, as well as a specific focus on carbon dioxide (CO<sub>2</sub>) concentration trajectories [[IPCC 2021b](#)]. The following scenarios are included in this analysis:

- **SSP1/RCP2.6:** emissions peak between 2040 and 2060, declining by 2100. This results in 3-3.5 °C of warming by 2100.
- **SSP2/RCP4.5:** emissions continue to increase through the end of the century, with resulting warming of 3.8-4.2 °C.
- **SSP3/RCP7.0:** models describe a large emission variability for this scenario. Warming in 2100 is estimated at 3.9-4.6 °C.
- **SSP5/RCP8.5:** high emissions scenario resulting in warming of 4.7-5.1 °C.

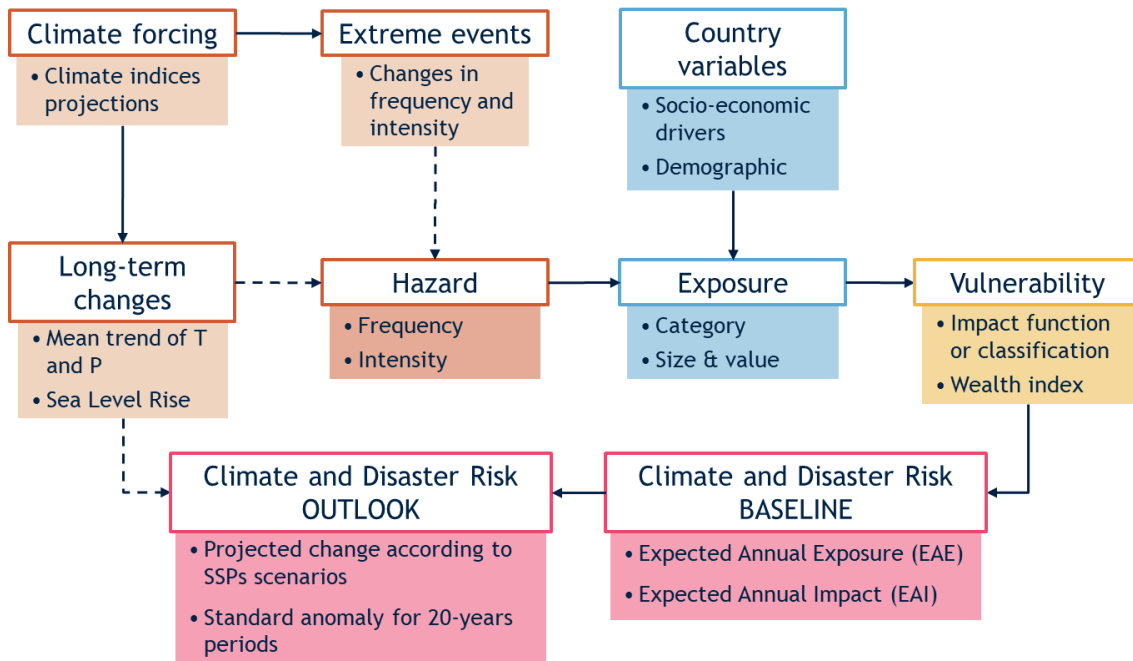
Each climate scenarios predicts different spatial patterns, resulting into a range of possible futures in terms of intensities, and frequencies of natural hazards. Key climate variables connected to the changing patterns of precipitation and temperature are collected from the [Copernicus Data Store](#) and summarized in *Table 2*.

*Table 2: Climate variables underlying climate projections*

Hazard	Associated climate indices	Unit of measurement
River and Pluvial Floods	Rainfall > 10 mm	Days per year
	Consecutive wet days	Days per year
	Maximum 5-day precipitation	mm
	Extremely wet days	mm
Coastal Floods	Sea Level Rise	m
Drought	Annual SPEI	Dimensionless
	Consecutive dry days	Days per year
Heat Stress	WBGT Heat index	Days per year > 23 °C
		Days per year > 30 °C

Figure 9 summarizes the theoretical workflow that is adopted in our analyses.

Figure 9: Workflow to estimate geographically disaggregated disaster risks

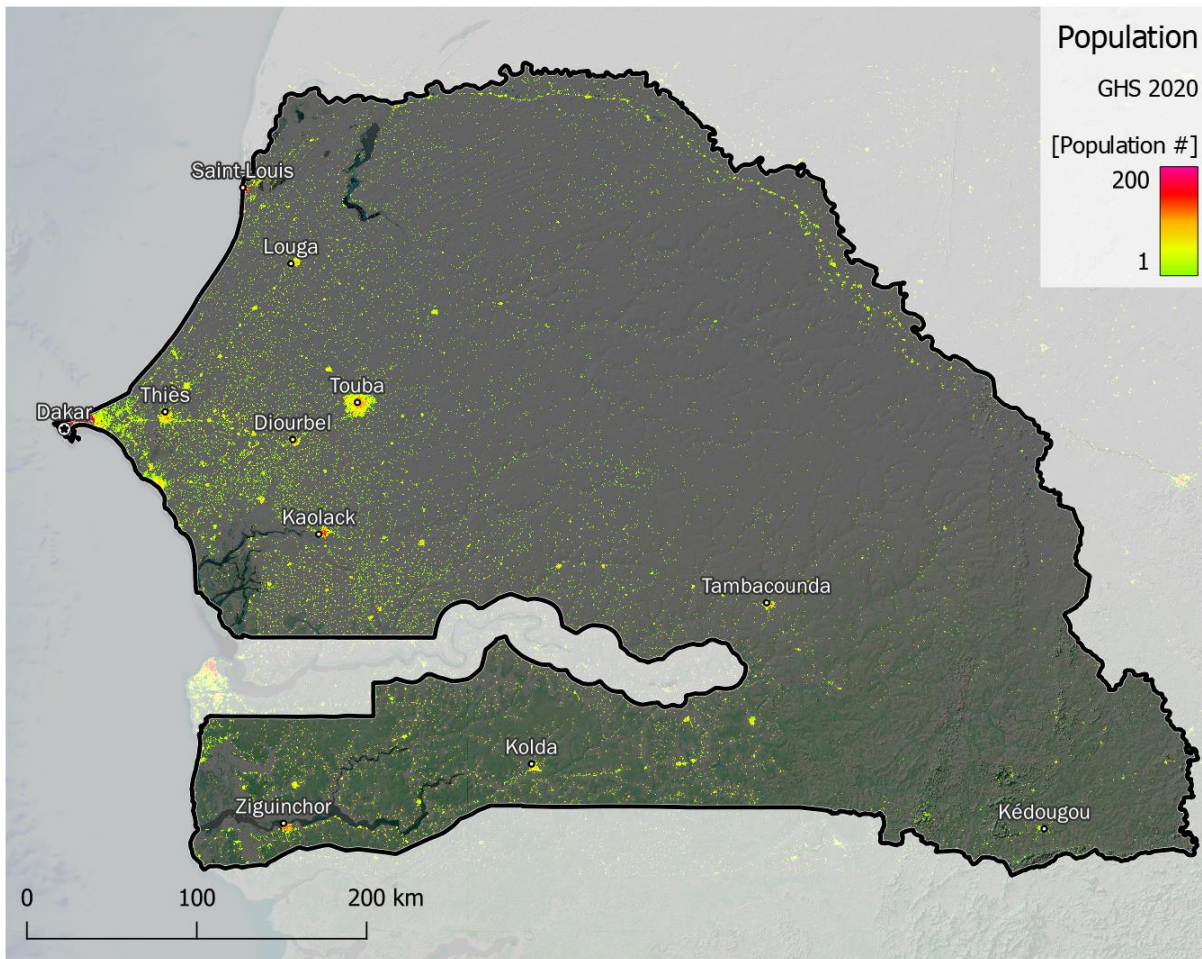


## 4 Exposure data

### 4.1 Population

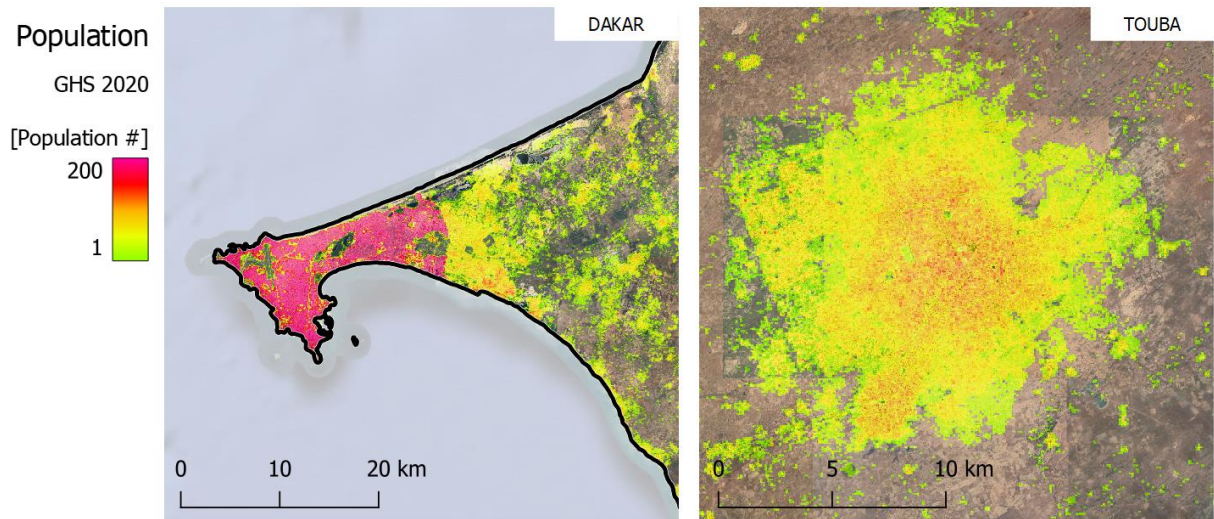
Whether an individual will be affected by a natural hazard depends on its location of residence. Population data at administrative levels (for instance from censuses) do not offer the required granularity to measure their exposure. Therefore, high-resolution population data from the Global Human Settlement population model [GHS-POP, [Schiavina et al. 2022](#)], with a 100-meter resolution, is used in the current analysis. *Figure 10* shows the distribution of the population across the country for the year 2020.

*Figure 10: GHS-POP 2020 population model for Senegal – 100 m grid*



As of 2022, Senegal's population was estimated to be approximately 17.9 million, with an annual growth rate of 2.7% [UN 2022]. The population of Senegal is concentrated in the western and coastal regions of the country, particularly around the capital city of Dakar (2.5 million residents, *Figure 11*). Some of the major urban centers include the cities of Touba (750,000), Thies (320,000), Kaolack (250,000), Ziguinchor (210,000) and Saint-Louis (200,000). In the northern regions of the country, population is located predominantly in the rural context.

*Figure 11: GHS-POP 2020 population for the urban area of Dakar (country capital) and the city of Touba (Diourbel)*

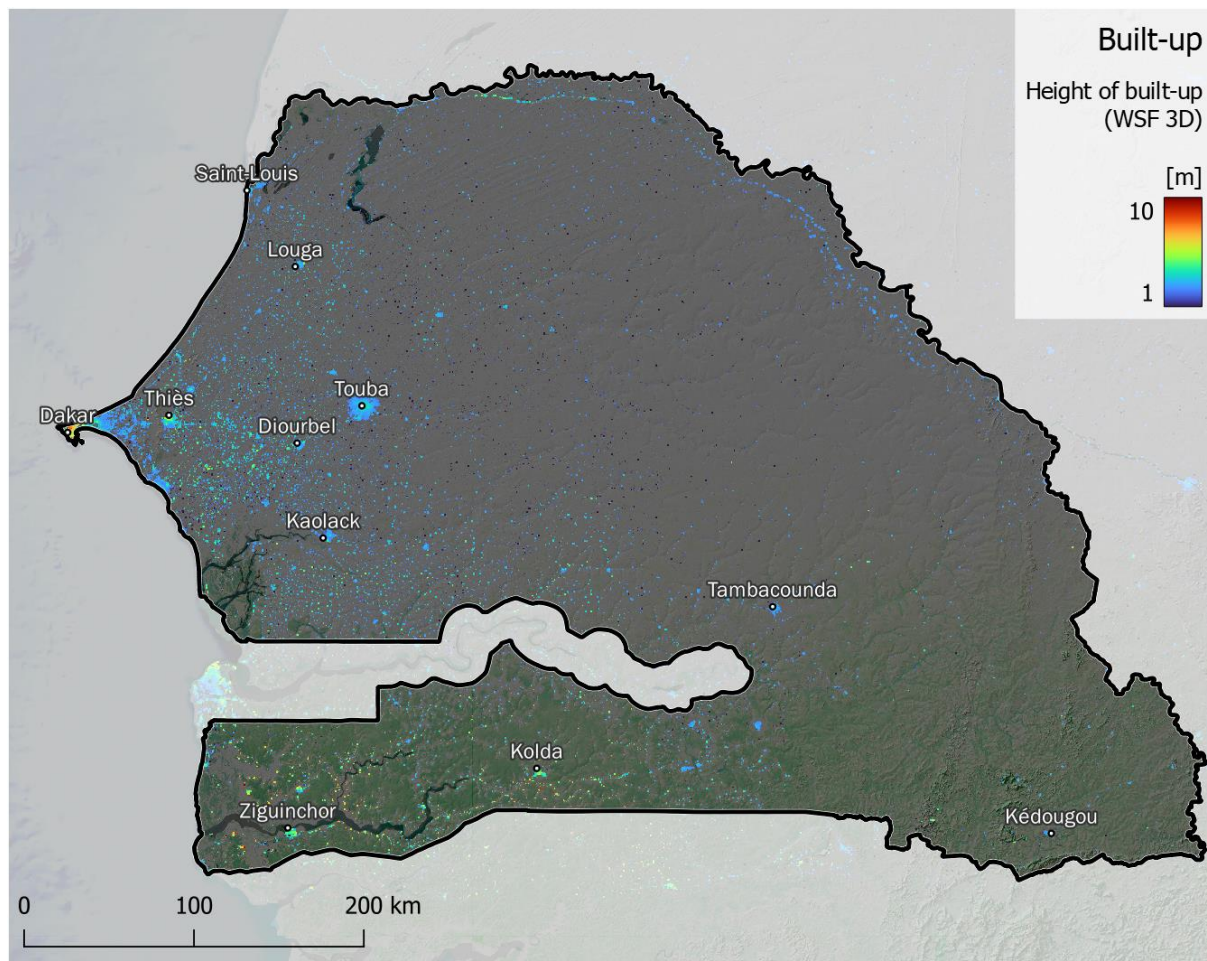


Note that high-resolution population mapping relies on census projections distributed in proportion to built-up density obtained from remote sensing data. This can induce model errors, particularly in mountainous and forest environments, resulting in an overestimation of natural hazard risk in those areas. The aggregation of exposure and impacts at the administrative level compensates for such biases to some extent, but residual errors cannot be ruled out suggesting careful interpretation of estimates is still warranted.

## 4.2 Built-up Assets

Built-up assets include homes, industrial complexes, road infrastructure, facilities, among other infrastructure. Data from [2019 World Settlement Footprint \(WSF\)](#) is used for this current analysis. The remotely sensed dataset includes WSF19, a 10-meter resolution layer of built-up presence for 2019, and WSF3D, a ~90-meter resolution layer representing the average height of buildings (*Figure 4*). Similar to population distributions, built-up assets are predominantly located in Senegal major cities, especially Dakar and its surroundings towns and villages. Numerous small villages are spread along the course of the main rivers.

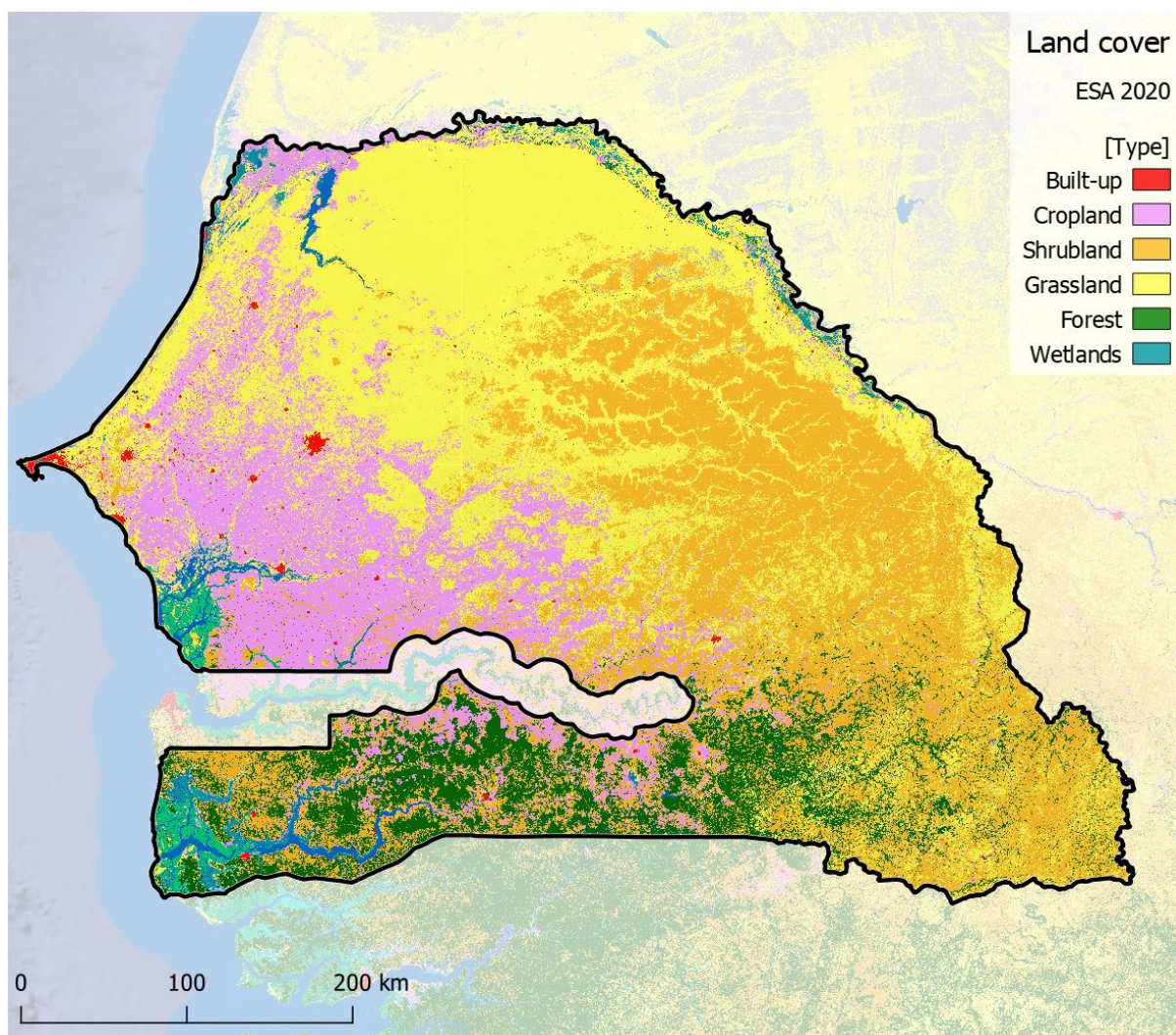
*Figure 4: WSF 2019 distribution of built-up area across Senegal*



### 4.3 Land cover

The [2021 WorldCover](#) dataset at 10m resolution from the European Space Agency is used to identify land cover types, in particular agricultural land where crops and livestock are located. The data are aggregated to 90m resolution and matched to the resolution of population model (*Figure 5*). The predominant land covers in Senegal are woody savannah (62%) and herbaceous vegetation (28%). Cropland covers about 6% of the country [EEA 2021]. Agriculture is the main economic activity in Senegal, accounting for around 16% of the country's GDP, and it is mostly located in the western regions and south-western regions. Crops grown include groundnuts, cotton, millet, sorghum, and rice. Additional datasets from FAO provide main crops ([GAEZ 2010](#)) and livestock ([GLW 2015](#)) distribution, that are considered in the drought risk analysis.

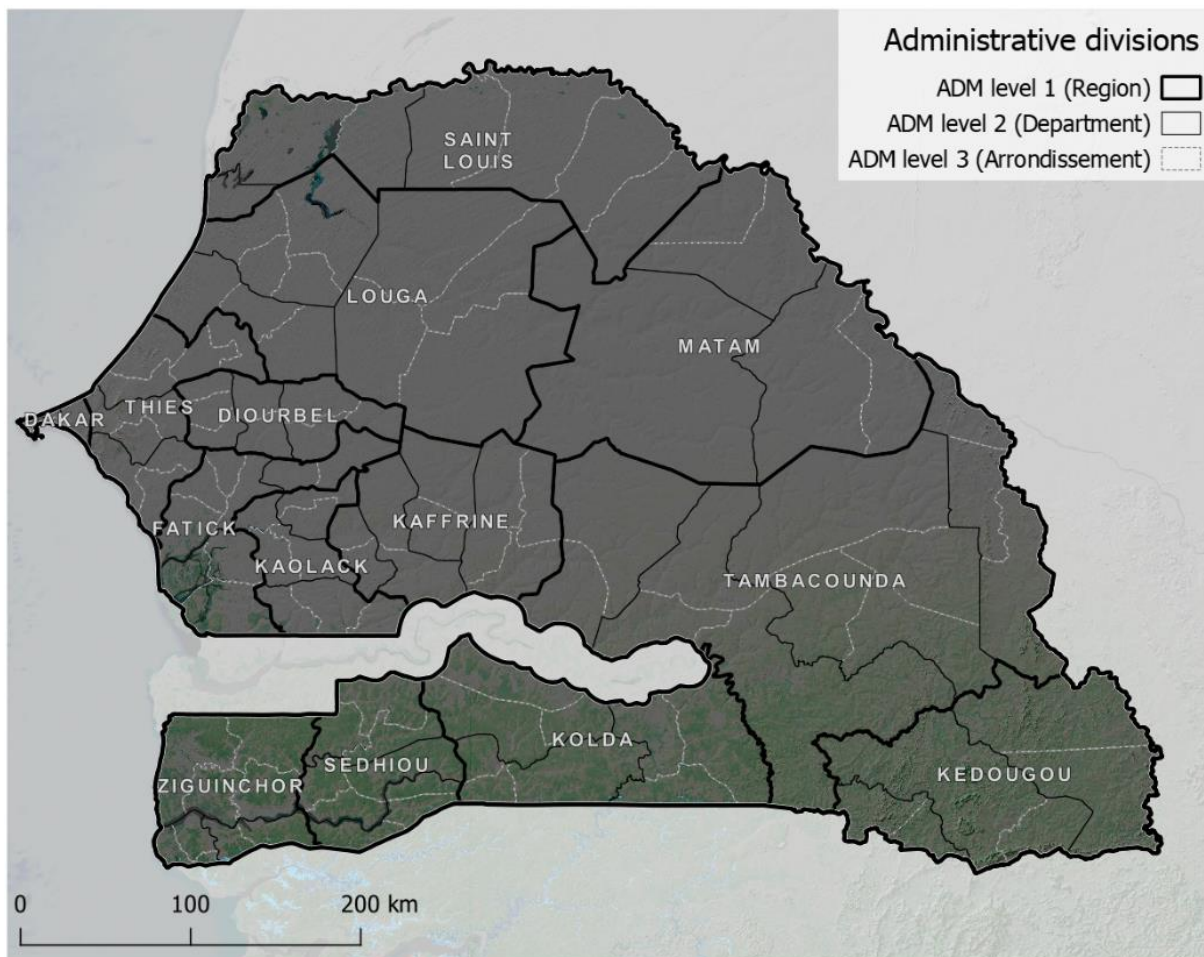
*Figure 5: ESA 2021 Land Cover across Senegal*



#### 4.4 Administrative boundaries

Senegal is divided into 14 regions (ADM level 1), which are further divided into 45 departments (départements, ADM level 2) and 103 arrondissements (ADM level 3). The ADM level 3 is used to summarize the results of the risk assessment.

Figure 6: Main administrative divisions of Senegal



## 5 Risk baseline: Mapping Hazard, Exposure and Vulnerability

The Expected Annual Impact or Expected Annual Exposure values are calculated following the combinations of available hazard, exposure and vulnerability models presented in *Table 1*.

### 5.1 Floods

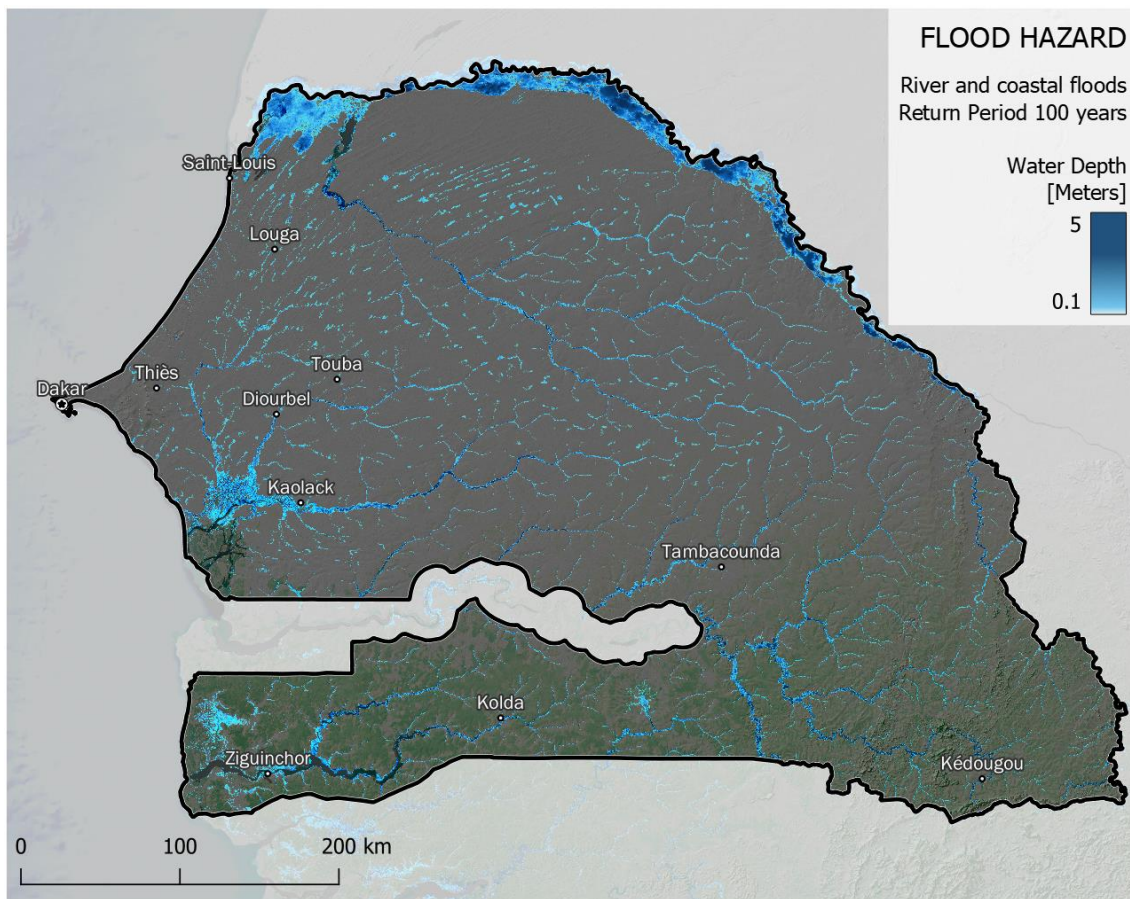
Flood is the most common and recurring disaster in Senegal, especially after the onset of the wet season (July to October). Major inland floods in Senegal have been recorded at an average of 1 to 3 years frequency [EMDAT 2023]. About 5,500 km<sup>2</sup> are flooded annually in Senegal, and 30% percent of this area is considered to be at high risk [[Bottazzi 2019](#)]. Each year, between 100,000 and 300,000 people are affected by floods that are exacerbated by poor urban planning and a lack of community awareness [[OCHA 2023](#)]. The most affected by these flood disasters were typically the urban areas, particularly the capital city of Dakar, where the infrastructure is often inadequate to handle heavy rainfall and the regions of Thiès, Louga and Saint-Louis [[OCHA 2022](#)]. It is important to differentiate: while fluvial (or river) floods originate from rivers exceeding their capacity, pluvial (or surface water) floods are a consequence of rainfall cumulation unrelated to the presence of water bodies, and strongly dependent on local conditions such as soil absorbing capacity and status of the drainage infrastructures; meaning that the same rainfall event can trigger very different risk outcomes depending on those parameters. For this reason, static hazard maps based on rainfall and DEM are unable to properly capture this kind of flood events. While less frequent than river and pluvial flooding, coastal flooding triggered by extreme sea levels and storm surges poses another major threat to Senegal populated coastal areas, especially the low-lying old capital of Saint Louis [[AFP 2021](#), [Cisse et al. 2022](#)].

The following is a review of some of the most severe flood events and related impacts since 2009. In September 2009, heavy rainfall caused serious flooding in Senegal, particularly in Dakar but also in the rest of the country. The flooding was not caused by exceptionally heavy rainfall but rather due to unfavourable existing conditions and the lack of a functioning stormwater drainage system. Based on the Post Disaster Need Assessment (PDNA), the event costed the country USD 104 million, including almost 56 million for damages and 48 million for losses. The peri-urban areas of Dakar were the most affected, with the cost of flooding estimated at 82 million USD. According to Government figures about 360,000 people were directly affected [[GFDRR 2009](#); [OCHA 2009](#)]. In September 2010, large areas in Senegal were affected by floods due to heavy rainfall, in particular the capital Dakar with its suburban areas (30,000 households). In September 2013, 163,000 people were affected by floods caused by heavy rainfall in Fatick, Kaolack and Thies regions as well as in the capital Dakar, where about half of the affected households is found. Three deaths have been reported in Thiadiaye and five in Dionksome, 94 people were injured. In the outskirts of the capital, six health centers out of nine have been seriously damaged [[OCHA 2013](#)]. Starting with the beginning of the rainy season in July 2012, torrential rains caused local flooding in several areas of Senegal, including St. Louis, Bambey and the capital Dakar. Over 6,500 houses were destroyed and more than 5,000 families were displaced [[OCHA 2012](#)]. Between July and September 2015, flooding from heavy rainfall caused significant damage in Dakar, Kaolak, Diourbel, Sedhiou, Kafrine, and Matam. Flood-affected households were estimated at over 100,000 people [[FAO 2016](#)]. In September 2016, a heavy rain floods affected 1,313 people in the area of St. Louis, especially the department of Dagana that recorded 5 deaths and 106 injured, in addition to destroyed houses and infrastructures. In addition, food stock reserves and livestock were lost in 4 towns and in the 44 towns and villages [[IFRC 2016](#)]. In September 2019, about 9,000 people have been

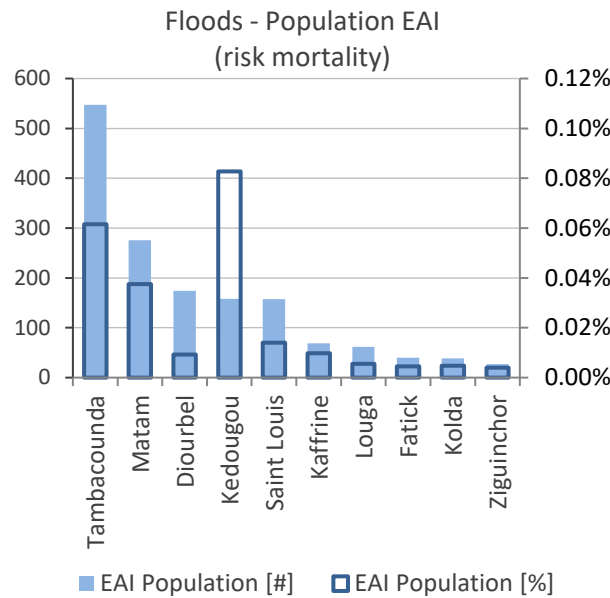
affected and around 4,500 displaced by heavy rain flooding in Rufisque and Guédiawaye departments (Dakar Region) and Kaolack department. Two people drowned in flood waters and almost 50 people were injured. Furthermore, the flooding has led to widespread destruction of livelihoods, as farms fields have been washed away [IFRC 2019]. The most affected people were women, children, the elderly, and people with disabilities who have been sheltered in schools with a limited access to essential services [IFRC 2020]. In September 2020, all regions of Senegal recorded an excess rainfall anomaly, affecting 11 regions (25 departments), causing the displacement of nearly 3,285 people in the suburbs of Dakar and the department of Thiès. The Senegalese Red Cross Society (SRCS) estimated about 17,000 people affected, among them 640 children under 5 years old, 216 pregnant/breastfeeding women, 72 people with disabilities, 533 elderly people [IFRC 2020]. In August 2022, the cities of Dakar, Thiès and Matam recorded heavy rainfall, resulting in the destruction of 170 houses and the displacement of 1,400 families. Three people died in the flood. The most affected were the five departments in Dakar, the department of Thiès, and two departments in Matam [IFRC 2022].

Figure 6 captures the geographic distribution of hazard intensity for river and coastal flooding events with a 100-year return period, according to the Fathom and Deltares global models. The Fathom dataset (undefended river floods) splits hazard potential into ten return periods, depicting how often flooding of a certain inundation depth occurs. The Deltares coastal floods dataset offers six return periods. According to the Fathom river flood model, potential flood depths up to 5 metres or more can be found in the floodplains along southern banks of the Senegal systems, where a constellation of small villages is located. Relevant flood extents are found along the Saloum river plain. The capital city Dakar is not affected by river floods, as it is located far from surface water bodies; however, it is frequently affected by pluvial floods.

Figure 7: River flood hazard across Senegal, Return Period 100 years

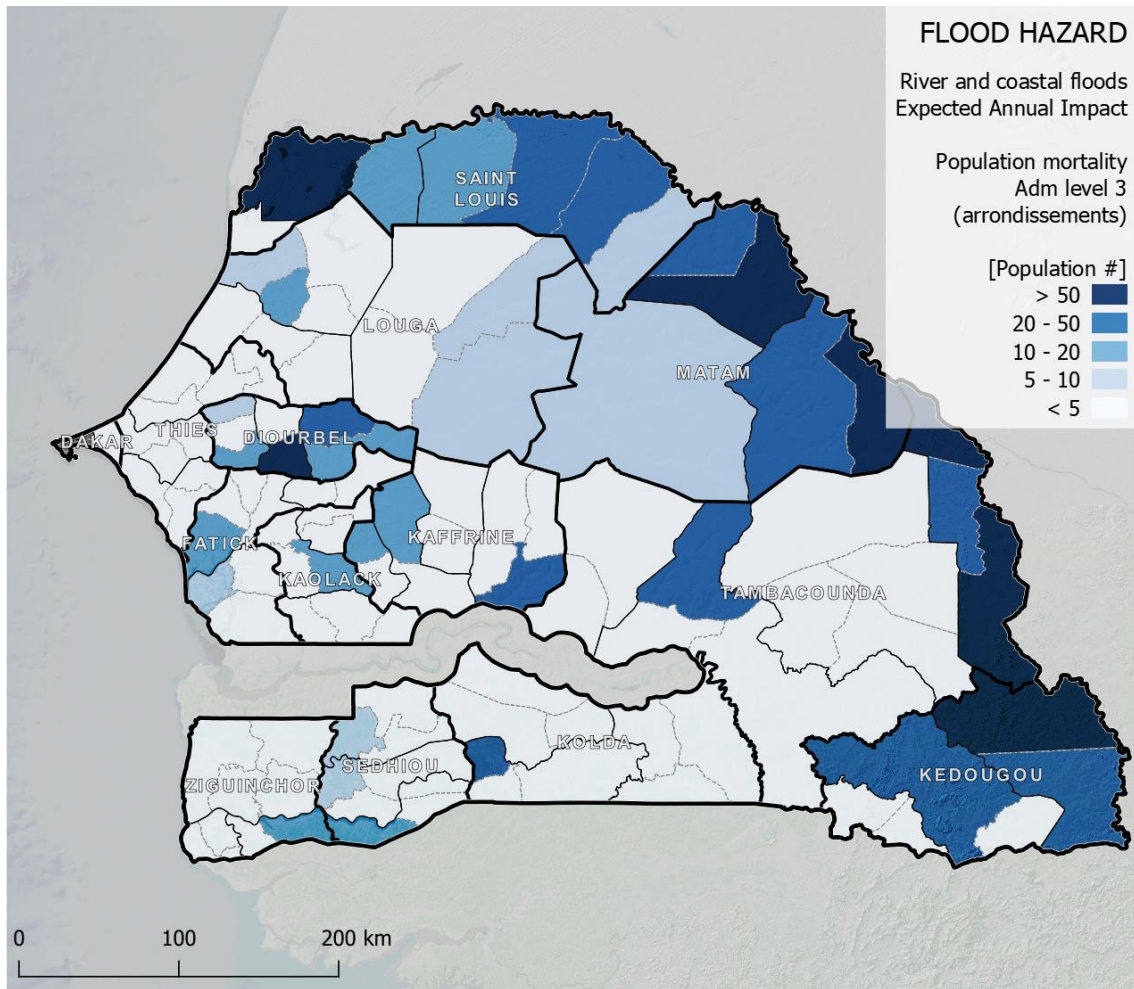


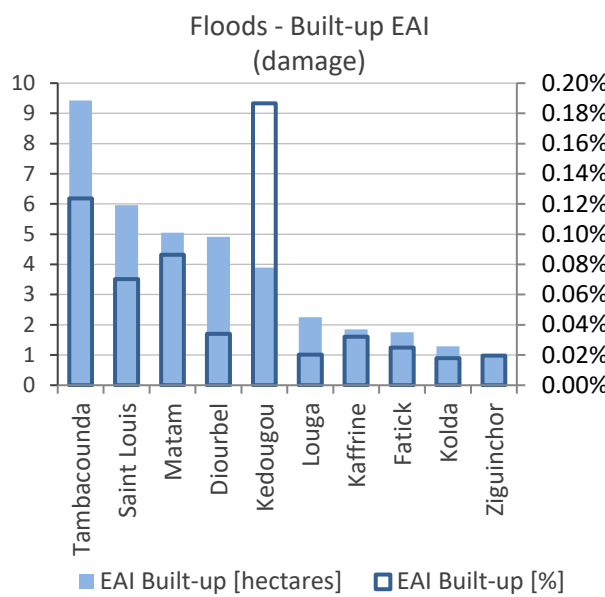
Expected Annual Impact (EAI) of floods in this analysis is calculated using impact functions and data on population and built-up area. EAI values are then aggregated at ADM3 level (arrondissements) for flood scenarios ranging from a return period of 5 years (frequent flooding event with low magnitude) to 1,000 years (extreme flooding event with high magnitude). Similar impact functions for agriculture are not available, therefore cropland exposure is expressed for water stages over 0.5 meter.



**Population:** the largest risk of mortality – above 100 people at risk of mortality every year – from flooding is found along the Senegal river systems, especially in Tambacounda (Bakel), Matam and Saint Louis, but also in other catchments, Diourbel and Kedougou (*Figure 7*). In comparison to the recent recorded events, the expected mortality values are comparatively larger in Tambacounda and lower in Dakar, Thiès and Kaolack. However, recent disaster records are mostly related to pluvial flood cumulation in urban areas, while this modelling refers to river overflow.

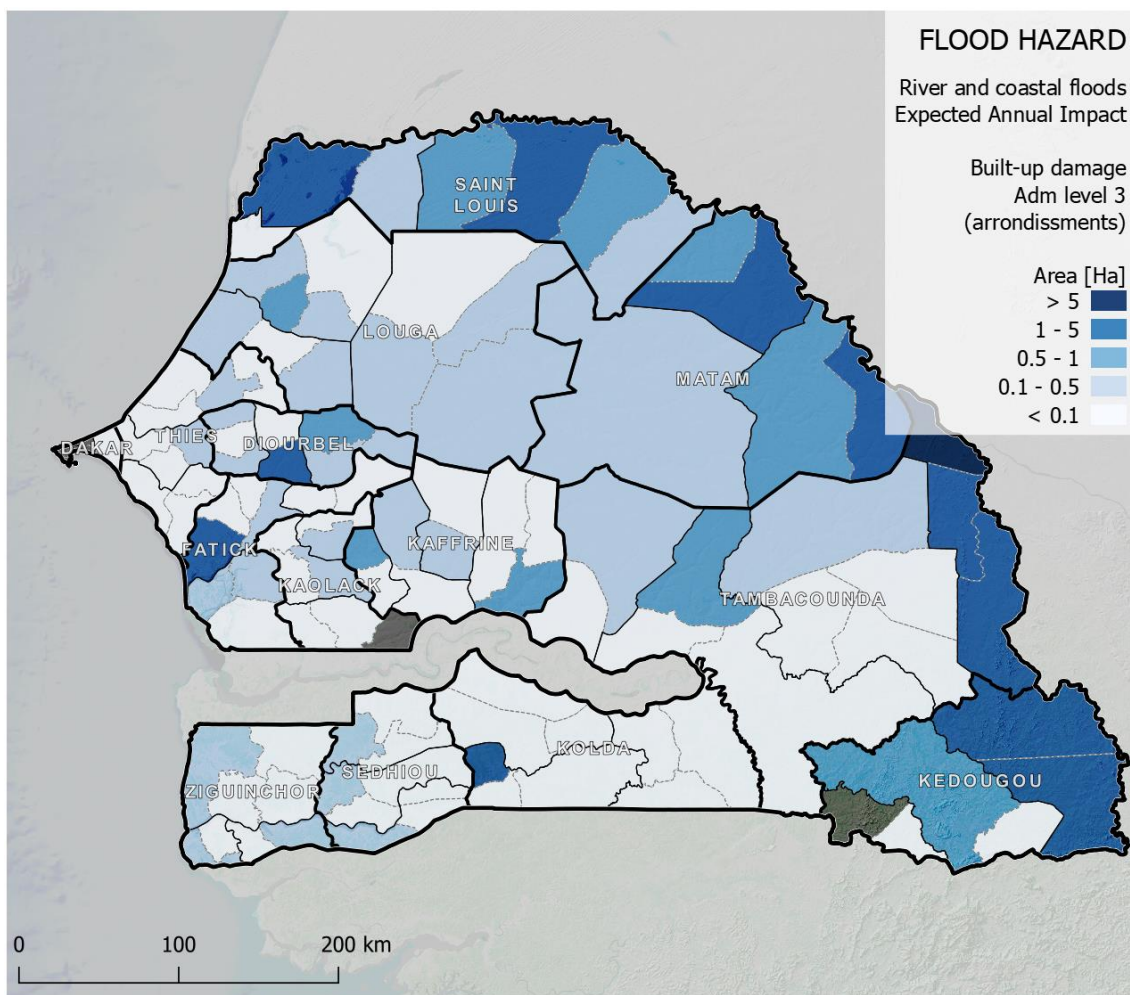
Figure 8: Expected annual impact of riverine and coastal floods on population mortality





**Built-up:** impact over the built-up (settlements and infrastructures) is largely distributed along the Senegal river similarly to population risk, except for Saint Louis, which shows much larger risk ranking due to large shares of asset exposed to coastal floods from storm surge events (*Figure 8*). Again, the arrondissement of Bakel in Tambacounda has the largest absolute risk score, followed by the town of Diourbel. The north-easter, scarcely populated region of Kedougou shows the largest relative impact (almost 0.2% of total built-up being at risk of total damage).

Figure 9: Expected annual impact of riverine and coastal floods on built-up damage (ha of built-up destroyed)



*Agriculture:* crop exposure is concentrated in Saint Louis, with almost 100 km<sup>2</sup> at risk for water depths above 0.5 m from river and coastal flooding; other regions along the Senegal river do not have much cropland. The western and south-western regions where majority of cropland is located are not exposed to intense flood events (water depth < 0.5 m) (Figure 9.), with over 60 hectares of agricultural land expected to be exposed to coastal flooding every year.

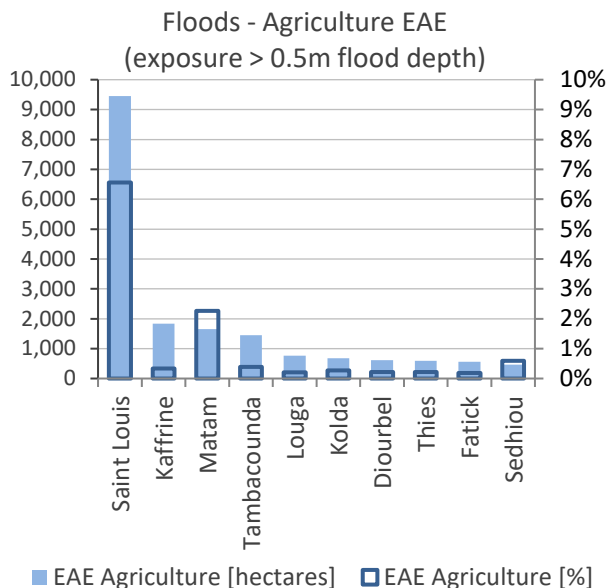


Figure 10: Expected annual exposure of agricultural land to riverine and coastal floods for water depth above 0.5 meters

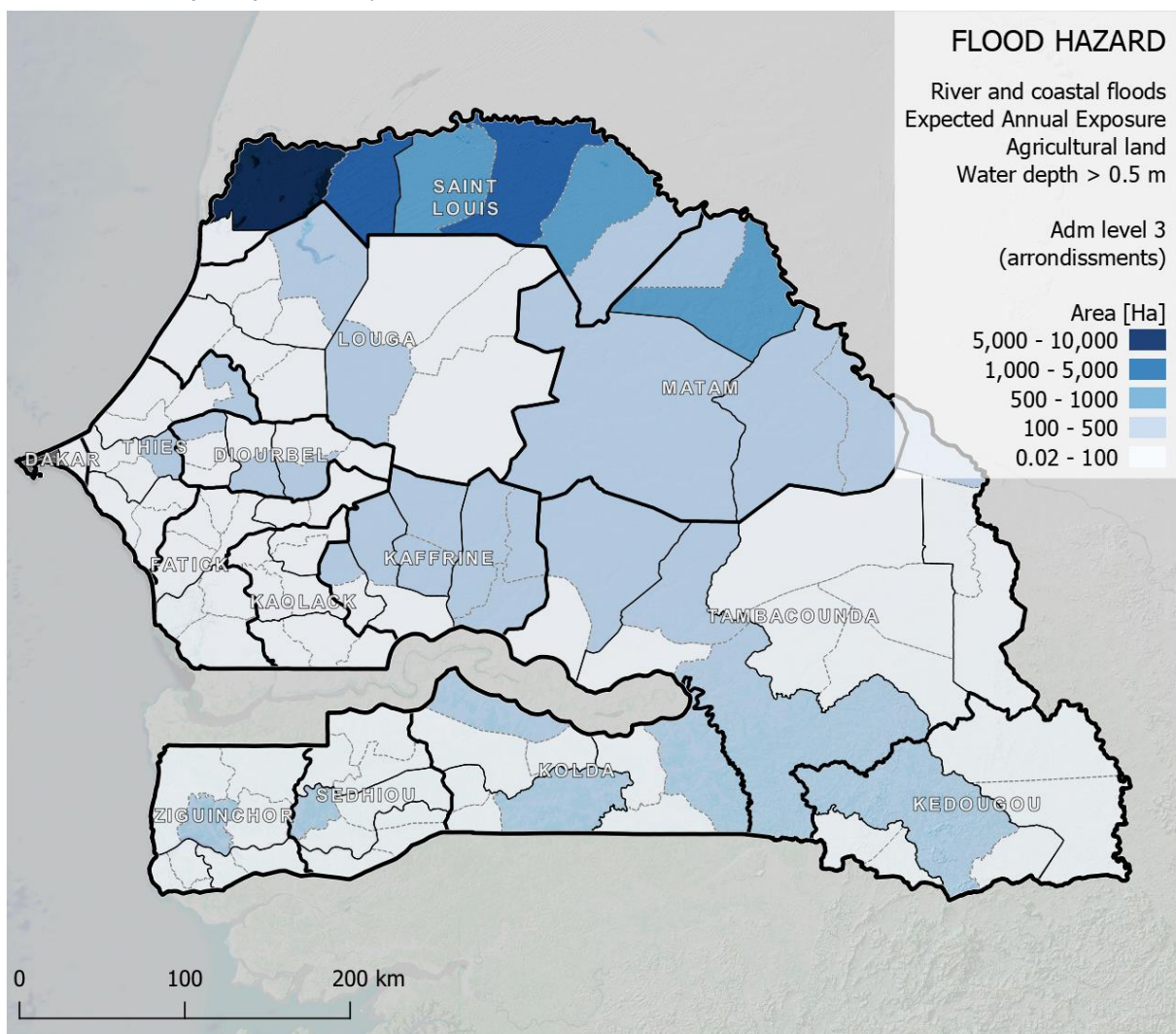


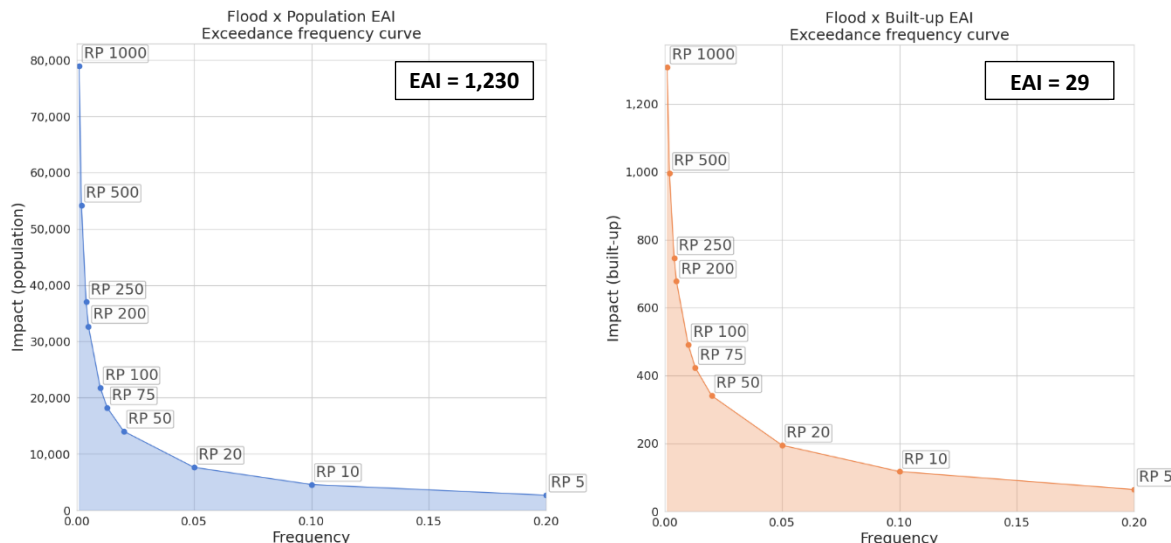
Table 3 presents the calculation of total EAI for population and built-up exposure categories, as explained in section 2.5.

Table 3: Expected Annual Impact from probabilistic analysis of flood risk over population and built-up (10 Return Periods).

Return Period [years]	Probability	Population impact [#]	Population EAI [#]	Built-up impact [ha]	Built-up EAI [ha]
5	0.2	2,689	269	64	6.4
10	0.1	4,577	229	117	5.9
20	0.05	7,629	229	195	5.8
50	0.02	14,048	94	341	2.3
75	0.013	18,221	61	424	1.4
100	0.01	21,807	109	491	2.5
200	0.005	32,666	33	678	0.7
250	0.004	37,006	74	747	1.5
500	0.002	54,194	54	996	1.0
1,000	0.001	78,976	79	1,309	1.3
Annual			1,230		29

The charts in Figure 10 show the Exceedance Frequency Curve for river floods over population (left) and built-up (right). The EAI for each category is calculated as the area below the curve: according to the models, on average, every year floods are estimated to put over 12 hundred people at risk of mortality from high floodwater levels, and to trigger a loss of built-up equivalent to 30 hectares destroyed. Note that both estimates are cumulative over the total value, e.g. 2 ha of built-up suffering 50% damage are summed up as 1 ha of built-up suffering complete damage.

Figure 11: Exceedance frequency curves for flood hazard over population (left) and built-up (right).



According to this data, largest impacts over population are expected from frequent flood events (up to 20 years return period), which seems consistent with the trend highlighted by the recent disaster records.

## 5.2 Agricultural drought

Senegal is geographically exposed to recurrent drought events, as its location within the arid Sahel region is characterized by low, erratic rainfall and high temperatures. These conditions can be worsened by climate phenomena such as the El Niño-Southern Oscillation (ENSO).

The country has experienced several drought events in the last 50 years, with the most affected regions being the north and northeast of the country. During the 1970s, Senegal experienced a severe drought that lasted for several years and caused widespread food shortages and famine [[FAO](#)]. The drought affected many regions of the country, particularly the northern regions within or bordering the Sahel. In 1983-1985, another severe drought affected Senegal and many other countries in the Sahel region, causing famine and massive displacement [[Timberlake 1985](#); [Findley 1994](#)]. The drought was caused by a combination of factors, including reduced rainfall, land degradation, and population growth. More recently, Senegal experienced severe drought conditions in 2011-2012, which affected over 800,000 people and led to significant livestock losses [[UN 2012](#)]. This drought was also exacerbated by the effects of the ENSO climate phenomenon. In 2017 [[OCHA 2017](#)], a drought event hit the Sahel, affecting several regions of the country, including Matam, Tambacounda, and Kolda, causing food shortages and loss of livestock. About 880,000 people were estimated to face acute food insecurity between June and August 2022, including nearly 9,000 people state of emergency. This is the highest number on record and well above the 490,000 people estimated to be acute food insecure during the same period in 2021 [[FAO 2022](#)]. The sharp increase is mostly associated to high food prices and poor livestock production in 2021 and the first half of 2022.

The current analysis uses drought probability estimates at from FAO's Agricultural Stress Index (ASI). The index measures the share of agricultural land (cropland and pasture combined) at a 1km resolution that is affected by drought annually between 1984 and 2022.

*Regional drought impacts:* the percentage of years over a 34-year period (1984 to 2022) during which at least one third (*Figure 11*) and half (*Figure 12*) of the cropland area was exposed to agricultural drought stress reveals that the most affected areas (dark orange in the map) are distributed along the northern border of the country. Saint Louis and Dakar are among the most affected units (severe droughts occurring every 8-9 years on average), followed by Thies and Diourbel. Fatick, Louga, Matam and Kaffrine are similarly exposed to moderate drought events (1/3 cropland affected), but the latter two show slightly more intense events (1/2 cropland affected).

Droughts - Frequency affecting cropland over the past 37 years

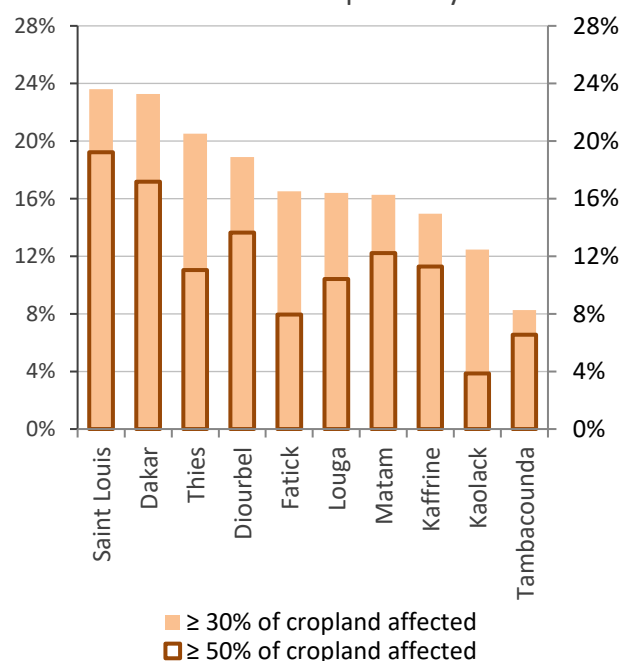


Figure 12: Frequency of drought hazard affecting at least 30% of crop across Senegal during the primary cropping season (April-October)

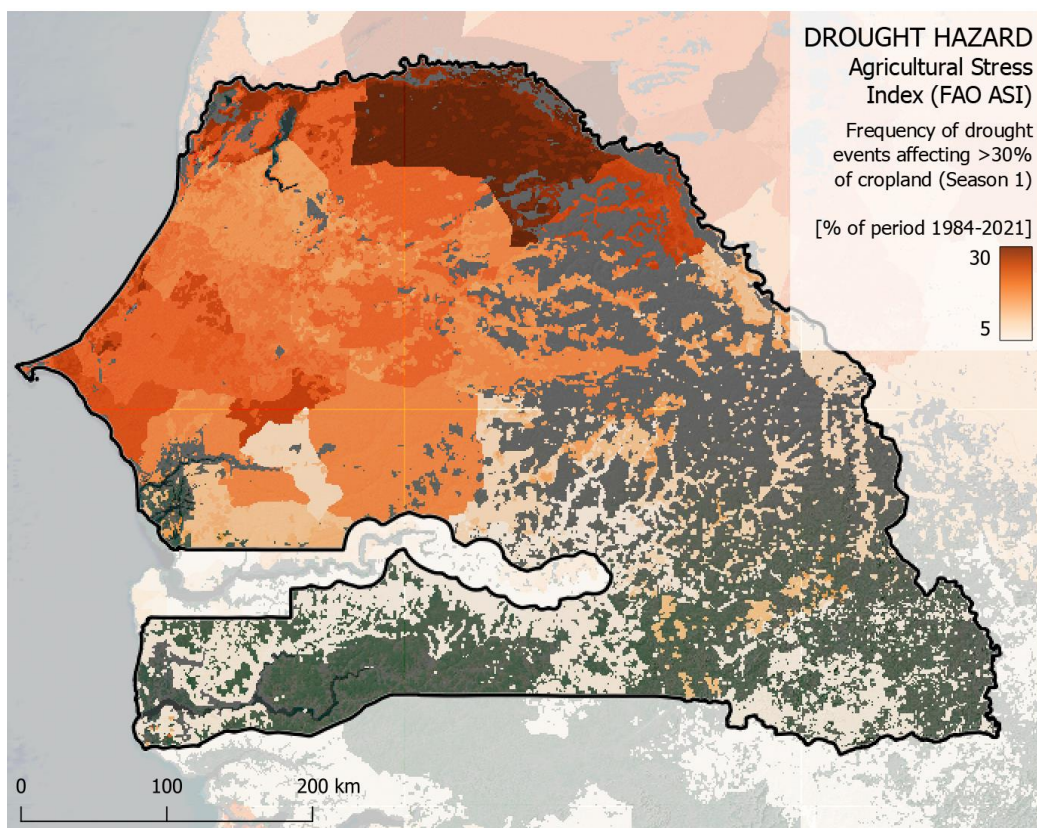
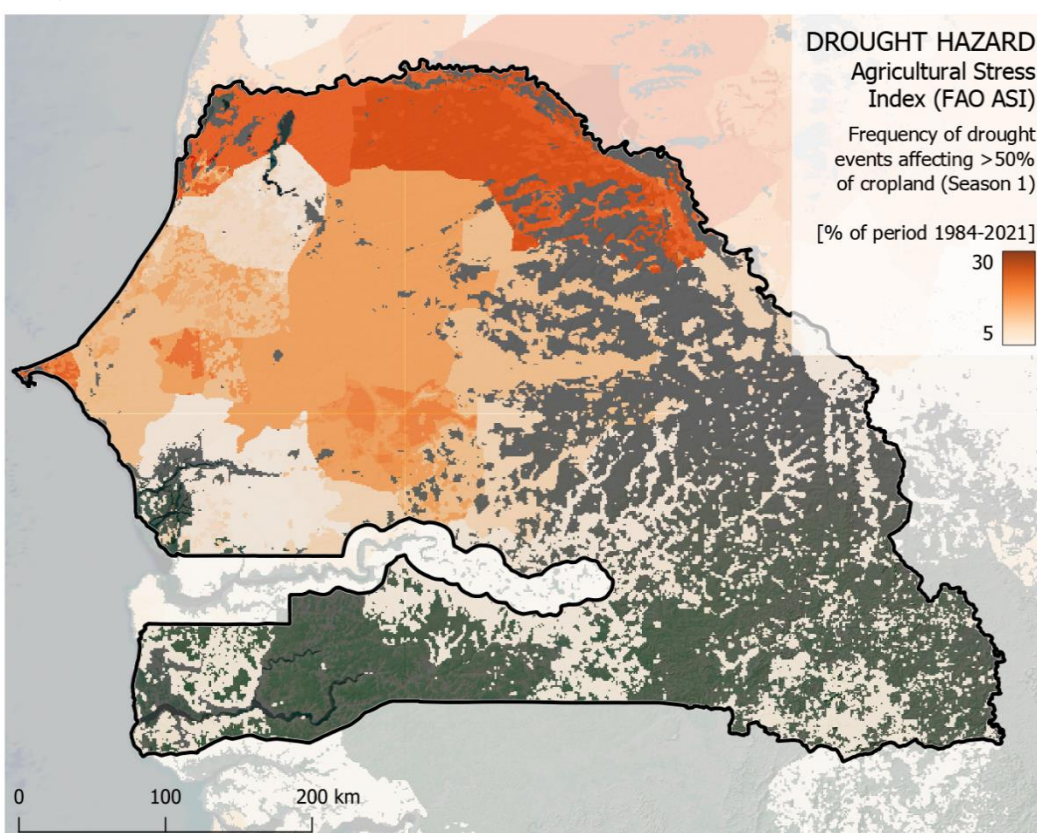


Figure 13: Frequency of drought hazard affecting at least 50% of crop across Senegal during the primary cropping season (April-October)



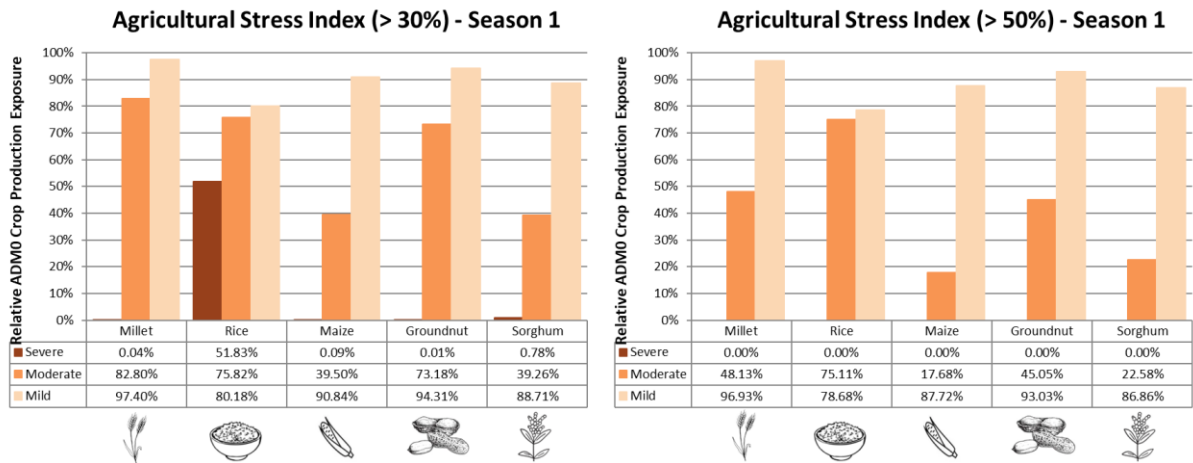
Groundnut (peanut) takes the individual largest share of cropland (up to 40% of arable land in some years), as former primary crop export (*Table 4*). Groundnut typically requires between 500 and 700 mm of rain to achieve good yields. The production is mostly located in central and western Senegal, north of the Gambia. Groundnut production employs about 7% of population. The most important subsistence crop is millet, one of the most drought-resistant cereals.

Table 4: main crop extent in hectares for the period 2021-2021 (FAOSTAT)

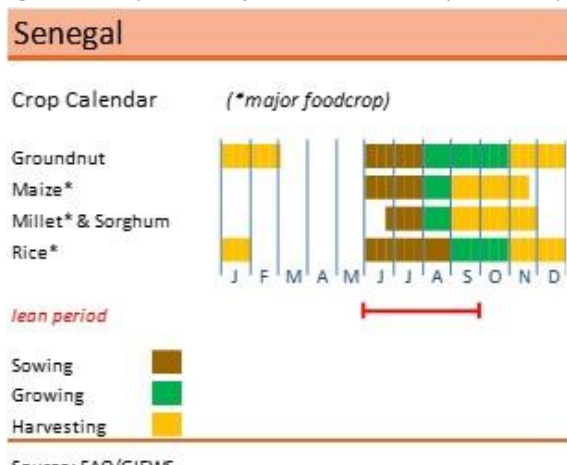
CROP	Area harvested [million ha]											
	2011	2012	2013	2014	2015	2016	2017	2018	2019	2020	2021	MEAN
Groundnuts	0.87	0.71	0.92	0.88	1.14	0.88	1.25	1.13	1.11	1.23	1.21	1.03
Millet	0.78	0.82	0.75	0.72	0.92	0.94	0.94	0.93	0.88	1.02	0.97	0.88
Rice	0.11	0.12	0.11	0.13	0.24	0.28	0.31	0.32	0.35	0.40	0.37	0.25
Maize (corn)	0.11	0.15	0.16	0.15	0.20	0.22	0.23	0.25	0.26	0.29	0.29	0.21
Sorghum	0.14	0.14	0.11	0.13	0.20	0.22	0.22	0.25	0.24	0.28	0.27	0.20

Figure 13 shows the historical exposure of main crops to drought according to FAO-GAEZ's 2015 crop distribution and the FAO's ASI mean value over the period 1984-2022. For 73% of the years in the timeseries (27 in 38 years), more than a third of groundnut crop is reported being affected by moderate drought conditions; in 45% of cases, more than half of cropland area was affected.

Figure 14: Agricultural stress index for droughts affecting over 30% and 50% agricultural land, primary season - Main crops



*Figure 15: Crop calendar for most common important crops*



*Figure 14* shows the calendar phases of the major food crops for the country. The main crops are aligned with their production cycles: most of the crop production cycle occurs between June and January, showing a slightly longer period in the south of the country compared to the north-west (*Figure 15*).

Figure 16: Start and end months of the main cropping season across Senegal. Season 2 production is limited to small areas in the Northwest

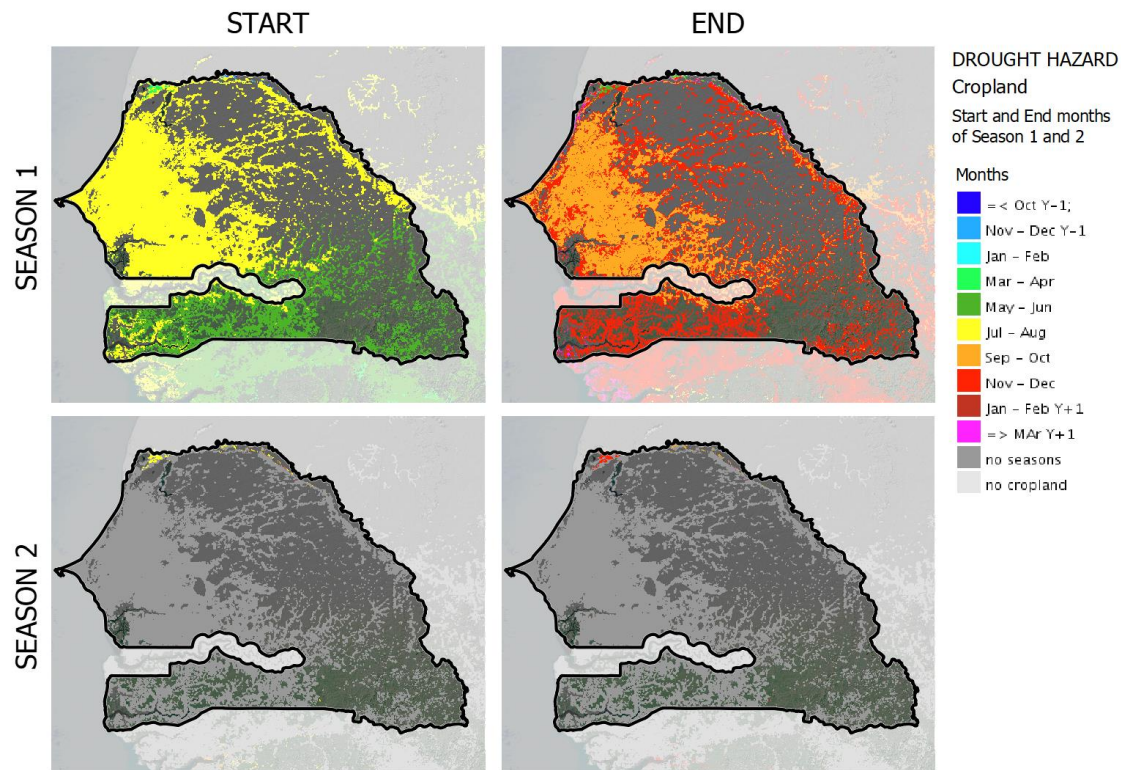
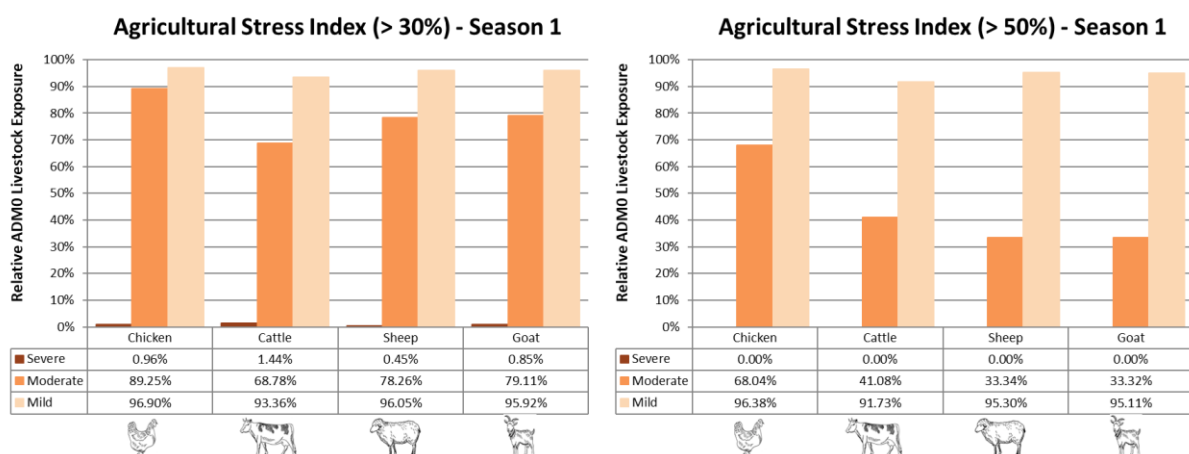


Figure 16 shows the historical exposure to drought according to FAO-GLW 2010 livestock distribution and the FAO's ASI mean value over the period 1984-2022. Poultry, goats, sheep and cattle make up are the most common farm animals. Poultry, goats and some types of sheep can withstand long periods with little water; cattle, on the other hand, suffers prolonged drought conditions. With the progression of the dry season, cattle breeders (pastoralists) are used to relocate their herd south, towards the Gambia border ([WB 2020](#)).

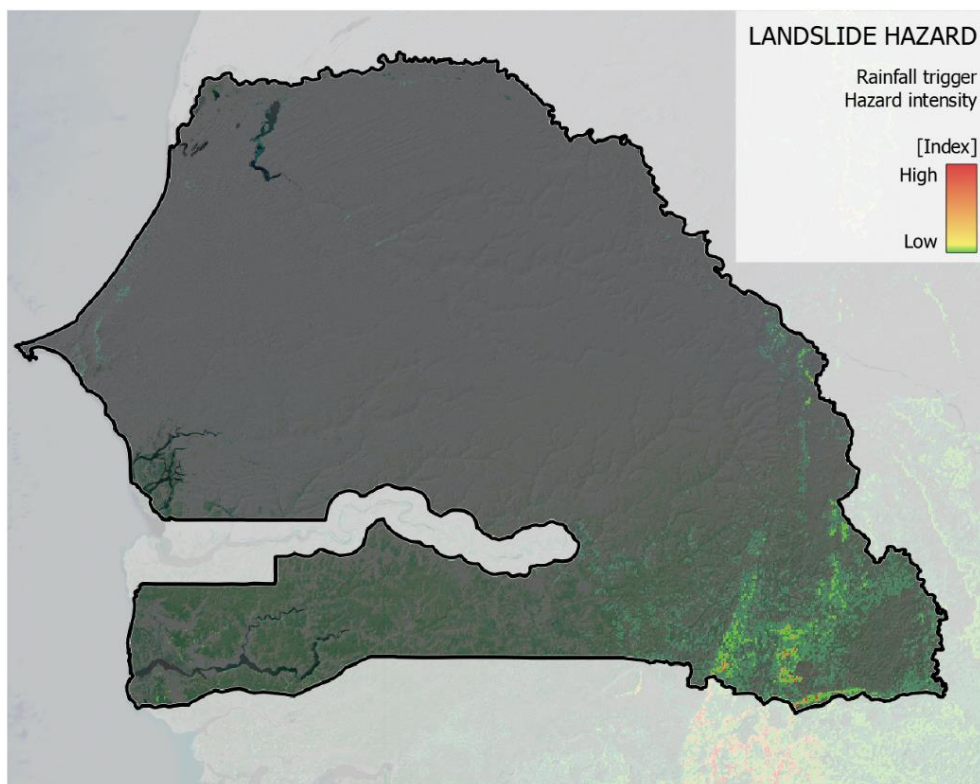
Figure 17: Agricultural stress index for droughts affecting over 30% and 50% agricultural land, primary season - Main livestock



### 5.3 Landslides

Extreme rainfall can temporarily alter water pressure within the soil causing soil slope to exceed its stability point, inducing landslides or mudslides. Land use change and deforestation can magnify the intensity of landslides. Landslide probability in this analysis is derived from World Bank-ARUP landslide hazard index available at 1km resolution (*Figure 17*). Landslide is not a frequent hazard in Senegal as the country does not have important reliefs and slopes: there is ancient massifs in the southeast of the country, reaching the maximum elevation of 581 metres near Népen Diakha; Kedougou. Additionally, a low relief and slope is located East of Dakkar (Thies Cliff), which have been ranked as very low to low landslide susceptibility [[Ndoye et al 2017](#)].

*Figure 18: Rainfall-triggered Landslide Hazard Index for Senegal at 1km resolution*



### 5.4 Heat stress

Human health is highly sensitive to the thermal environment [[WHO 2008](#)]. Extreme heat events lead to heat stress and can increase morbidity and mortality [Garcia-Herrera et al 2010, NOAA Watch 2014] as well as losses of work productivity [[Kjellstrom et al 2009](#), [Singh et al 2015](#)]. Heat waves can cause long-term impairment to learning capacity and reduce labour productivity and incomes [[Goodman et al 2018](#)]. Heat discomfort increases when hot temperatures are associated with high humidity [[Coffel et al 2018](#)]. Not everyone reacts to the heat stresses in the same way, as individual responses are conditional on their medical condition, level of fitness, body weight, age, and economic situation [National Institute for Occupational Safety and Health 2016]. The current analysis focuses on the impact of heatwaves on health. Senegal is exposed to high annual average temperatures, which climb up over 35°C during the dry season, especially in the north. In this report, heat stress probability is measured by the Wet-Bulb Globe Temperature (WBGT in °C). The WBGT combines temperature and humidity, both critical components in determining heat stress. Three return periods of heat events are included in the analysis: once in 5, 20 and 100 years.

Figure 19: Heat stress across Senegal according to WBGT °C for a heat event with 20-year return period

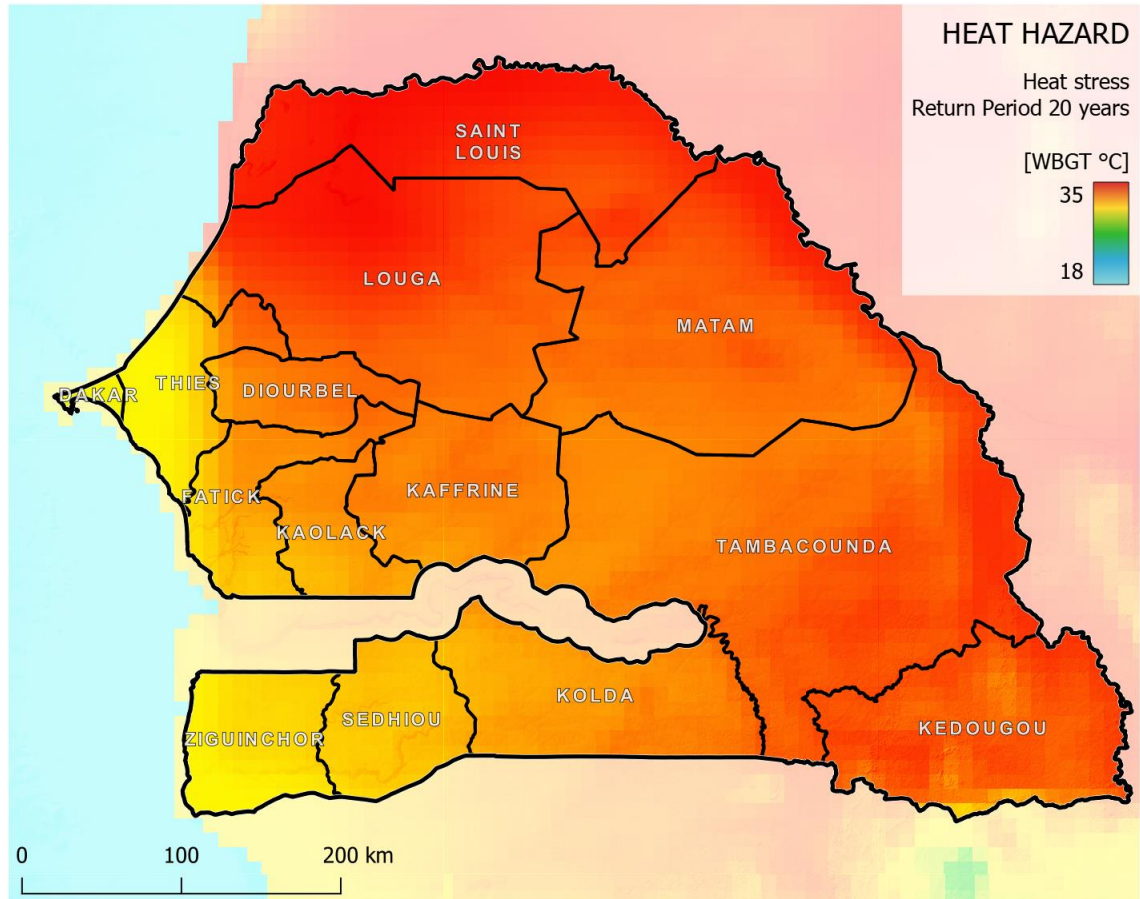
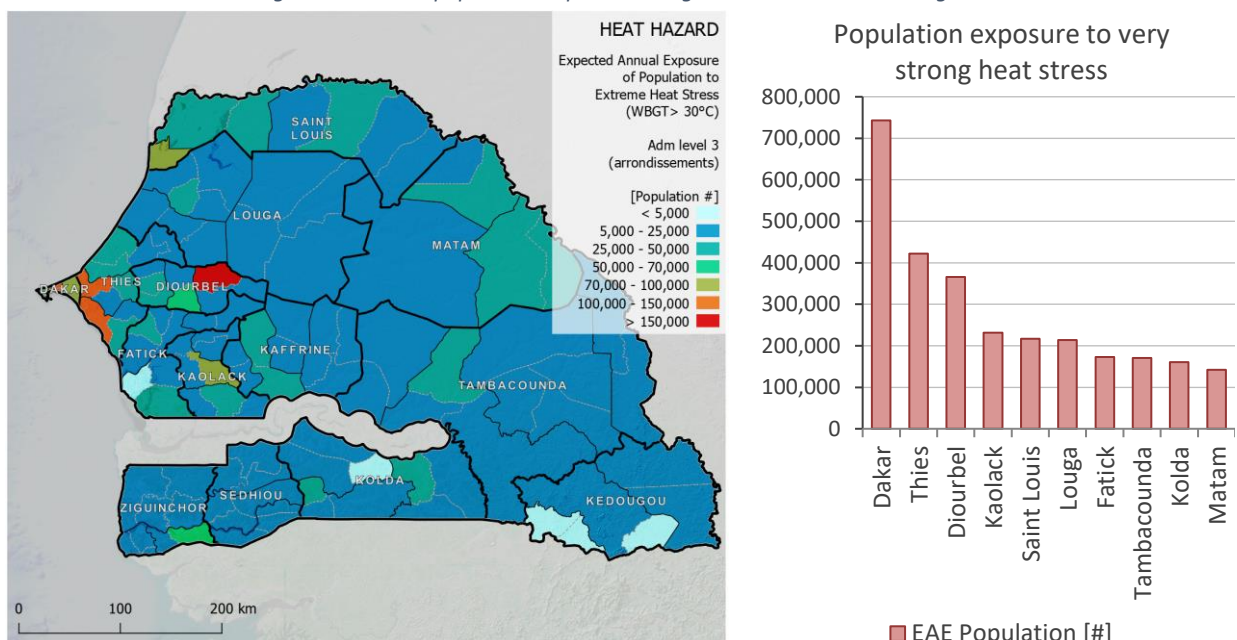


Figure 29 represents modelled maximum heat for the 20-years return period scenario. WBGT values above 33 °C are estimated in Saint Louis, Louga and Matam. Figure 18 shows the annual expected population exposure combining all the hazard probability scenarios. Several hundred thousand people, especially those in dense urban centres (Dakar, Thiès, Touba) face exposure to extreme heat stress on an annual basis, with severe health and economic implications.

Figure 20: Annual population exposure to high heat stress across Senegal.



## 5.5 Air pollution

Air pollution is measured by the mean annual surface-level concentrations of PM<sub>2.5</sub>, which is available from 1998 to 2020 [[van Donkelaar et al, 2021](#)] at 1.1km spatial resolution. This dataset combines data from different sources, including NASA MODIS, MISR, and SeaWiFS observations with the GEOS-Chem chemical transport model into a high-resolution map of air pollution. The dataset combines both human-induced PM<sub>2.5</sub> emissions, emitted, for instance, by car engines, power plants, as well as fireplaces and biomass burning [[NCRD 2014](#)] and natural sources of PM<sub>2.5</sub>, which include forest fires and desert dust [[McDuffie et al. 2021](#)]. These fine particles, smaller than 2.5 micrometers in diameter, pose enormous health risks as they can lodge deeply into the lungs [[WHO 2019](#)]. Concentrations of PM<sub>2.5</sub> over 15 µg/m<sup>3</sup> can lead to severe public health consequences (respiratory infections, cardiovascular disease, and lung cancer), especially in densely populated areas. While not a climate hazard in and of itself, air pollution can be affected by climate change [[UCAR 2022](#)], but can also affect local climate: drier conditions can promote dust transport from soil; wildfires can increase the local dust concentration; high dust can alter the heat intake from the sun and thus affect temperatures. *Figure 19* depicts the average 1998-2019 concentration of fine particulate matter (PM 2.5) in Senegal. Linking pollution hazard to population exposure and using the mortality impact function associated with high PM<sub>2.5</sub> concentrations (*Figure 20*) helps to better identify places with the largest absolute number of people exposed to health issues and reduced life expectancy. The exposure is found to be higher in the densely urbanized areas of Dakar, Thiès and Diourbel (more than 350 thousand people affected), followed by other large cities. Overall, approximately 4 million people (almost 24% of the country population) are exposed to health impacts from air pollution.

*Figure 21: Air pollution hazard (mean PM 2.5) across Senegal*

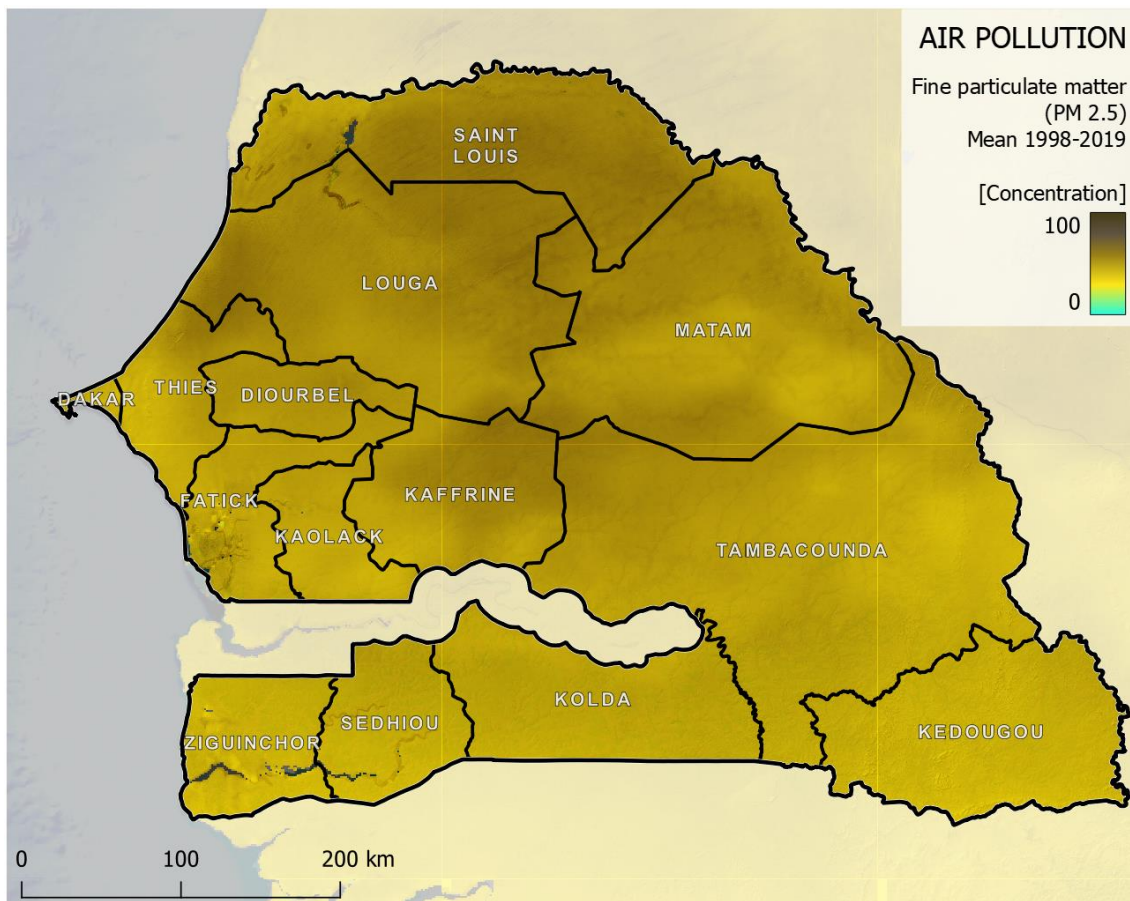
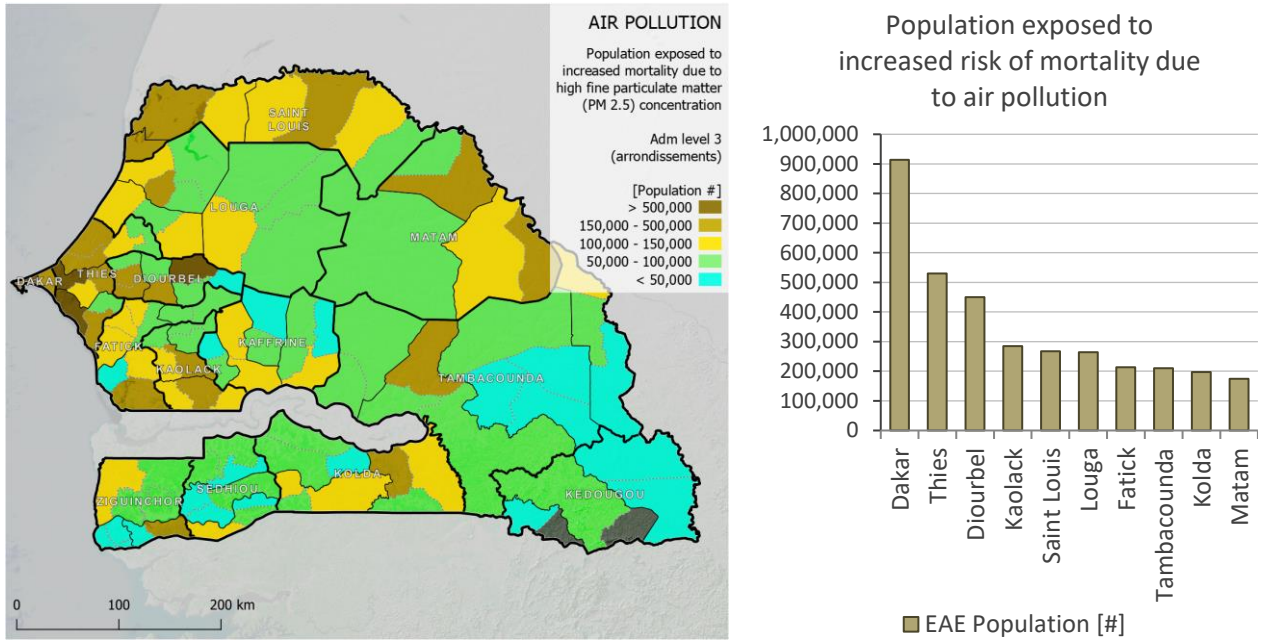


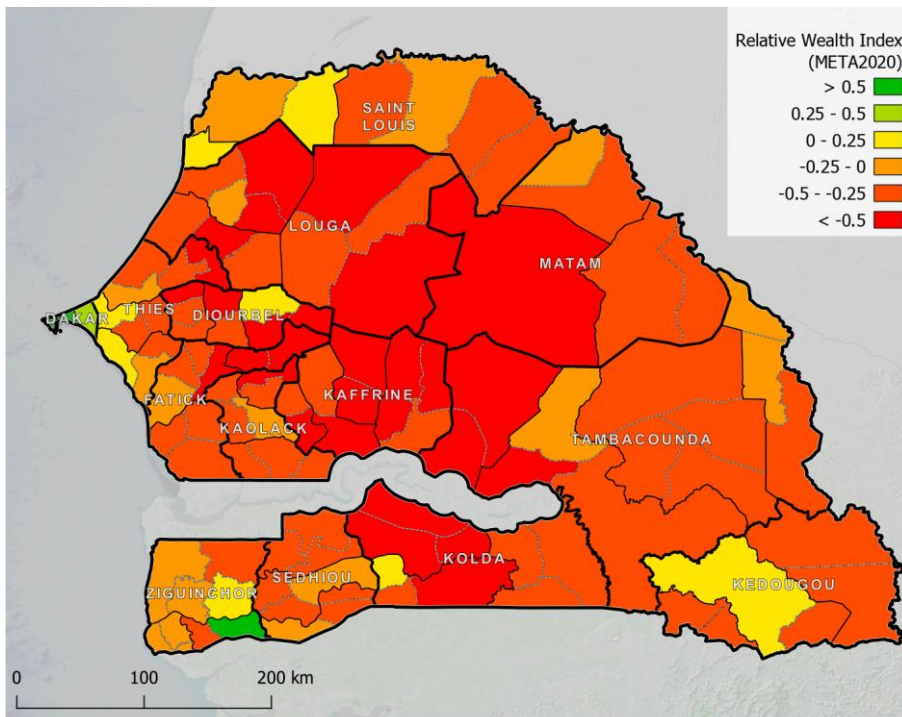
Figure 22: Air pollution impact over population across Senegal



## 6 Risk and Poverty – Bivariate maps

The distributional impact of climate risks can be examined by overlaying poverty maps shown in Figure 21, on built-up asset and agricultural land EAE and EAI maps produced in the earlier section. These results are visualized using a series of bivariate maps that show the locations where risk is most likely to translate into severe impacts on the poorest and vulnerable households.

Figure 23: share of population living in poverty conditions in 2020 based on poverty maps for ADM3 level (Communes).



Relative poverty maps are produced based on the RWI 2020<sup>3</sup>. The RWI values are weighted using the population layer to make the index demographically representative [Filmer and Pritchett 2001] before calculating the average for sub-national administrative units (ADM3 level). These are combined with the risk maps (EAE or EAI) at the same level to obtain bivariate maps. The bivariate maps provide ranks explained by a 3x3 matrix, resulting in 9 possible scores ranging from low-risk / low-poverty to high-risk / high poverty. The matrix is built by classifying poverty indicators into three quantiles and dividing risk indicators (EAE or EAI) of each hazard type into classes, as shown in *Table 5*. The thresholds are expert-based and country-specific. The units falling in the higher risk and poverty classification are highlighted in red and labelled in the maps.

*Table 5: Selected risk classification approach by hazard*

Risk indicator	Unit	Risk Classification		
		Low	Medium	High
River Flood x Population	EAI [#]	0.01 – 1	1 – 10	> 10
River Flood x Built-up	EAI [Ha]	0.001 – 0.1	0.1 – 0.5	> 0.5
River Flood x Agri land	EAE [Ha]	0.01 – 50	50 – 250	> 250
Coastal Flood x Population	EAI [#]	0.01 – 1	1 – 5	> 5
Coastal Flood x Built-up	EAI [Ha]	0.001 – 0.01	0.01 – 0.1	> 0.1
Coastal Flood x Agri land	EAE [Ha]	0.01 – 1	1 – 25	> 25
Drought x Agri land	EAE [Ha]	1 – 5	5 – 15	> 15
Heat stress x Population	EAE [#]	1 – 10,000	10,000 – 25,000	> 25,000
Air pollution x Population	EAE [#]	1 – 50,000	5,000 – 100,000	> 100,000

The expected annual impact of river floods on population mortality (*Figure 22*), damage to built-up assets (*Figure 23*) and annually exposed cropland and pasture (*Figure 24*) is overlaid with relative poverty maps as described in chapter 2.6. The arrondissements of Keur Mbouck and Ida Mouride fall in the high risk / high relative poverty category both in terms of population mortality and built-up damage. In comparison, the populated areas along the Senegal river have similar risk levels, but higher relative wealth. Poorer households are more likely to reside in hazard-prone areas, with poorer insurance and adaptive or preventive measures against high water.

*Figure 24: Expected annual impact from river flood hazard over population in relation to wealth (RWI)*

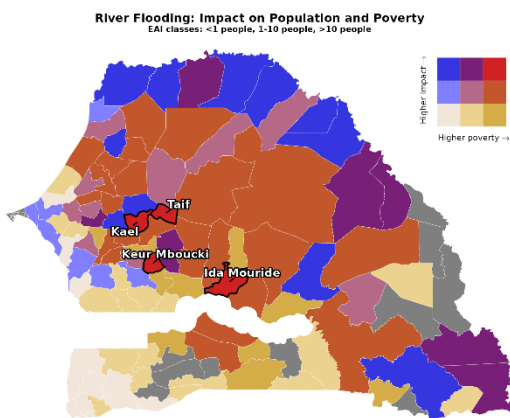
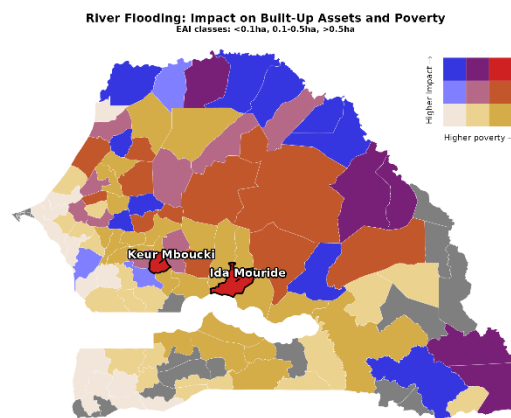


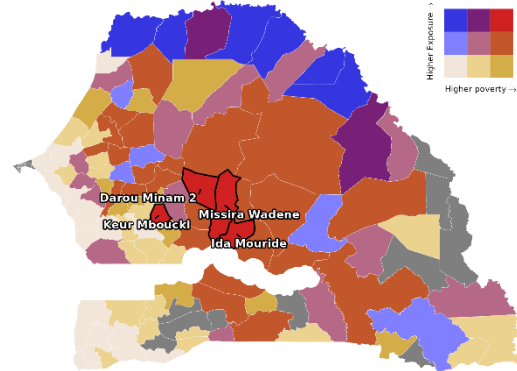
*Figure 25: Expected annual impact from river flood hazard over built-up in relation to wealth (RWI)*



<sup>3</sup> See the annex for details about RWI processing.

*Figure 26: Expected annual impact from river flood hazard over agricultural land cover in relation to wealth (RWI)*

River Flooding: Exposure of Agricultural Land and Poverty  
EAE classes: <50ha, 50-250ha, >250ha



The effects of flooding on agricultural land and poorest households are concentrated in the central parts of the country. Farmers located in these regions face high flood risk while having likely less capacity to respond to it or take adaptive measures.

Similarly, here the coastal flood risk maps are overlaid with the relative poverty maps. The pattern is similar for the three exposure categories, with the largest hazard risk occurring on the very coast, while the relative poverty increases in the innermost Saloum and Gambia delta regions.

*Figure 28: Expected annual impact from coastal flood hazard over built-up in relation to wealth (RWI)*

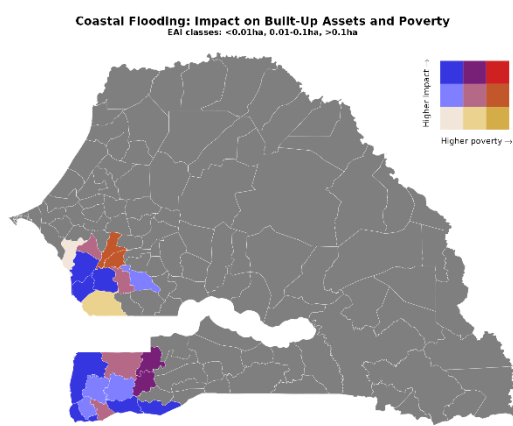


*Figure 27: Expected annual impact from coastal flood hazard over population in relation to wealth (RWI)*

Coastal Flooding: Impact on Population and Poverty  
EAI classes: <1 people, 1-5 people, >5 people

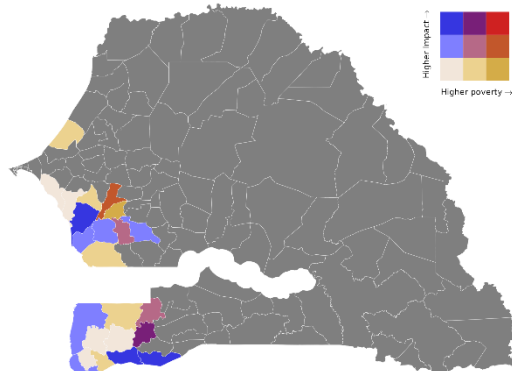


*Figure 29: Expected annual impact from coastal flood hazard over agricultural land cover in relation to wealth (RWI)*

Coastal Flooding: Exposure of Agricultural Land and Poverty  
EAE classes: <1ha, 1-25ha, >25ha

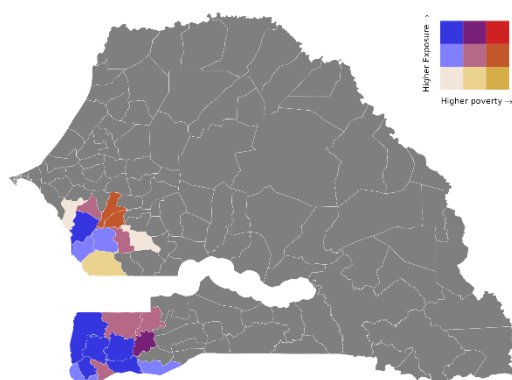
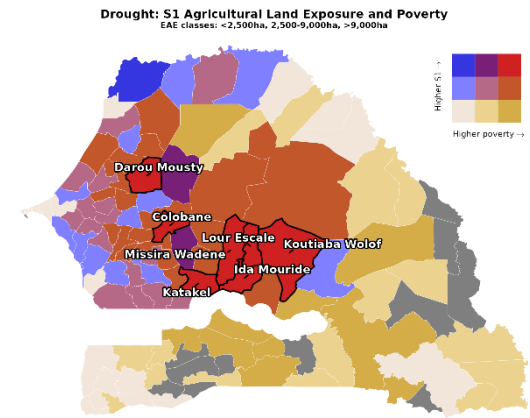


Figure 30: Expected annual exposure of agricultural land to drought in relation to wealth (RWI)



Recurring drought events can affect large areas of the Senegal territory, and their impact can be more severe in lower wealth areas in the centre of the country, north of the Gambia (Figure 25). The south and south-east area have high relative poverty, but low hazard occurrence. Oppositely, the western and northern region show higher drought risk values, but lower poverty rates.

With the exception of settlements located along or near the Atlantic coast, heat stress occurs throughout the country and affects nearly all Senegalese with relative high frequency and intensity. The northern areas are the most exposed to intense heat stress, yet the relatively higher wealth scores and the presence of the Senegal river can partially compensate for the heat risk. The innermost areas show medium to high heat stress risk and relatively lower wealth distribution (Figure 26). The communities in these areas are most at-risk of the negative health consequences of extreme heat stress. The densely populated urban centres such as Dakar and Saint Louis are comparatively less exposed to heat stress and have more means to cope with their impact. However, [heat island effect](#) can increase the intensity of extreme temperature events, and this is not accounted by the hazard model.

Figure 31: Expected annual exposure of population to heat stress in relation to wealth (RWI)

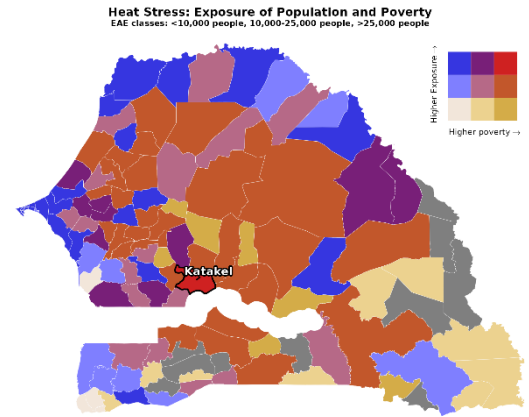
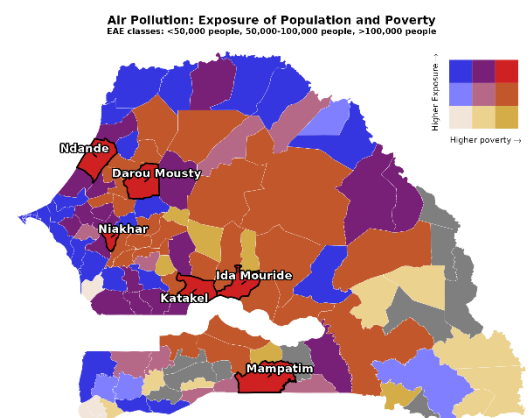


Figure 32: Expected annual impact from air pollution on population in relation to wealth (RWI)



Air pollution hazard is widespread in the country, due to dry conditions and the presence of desert dust (Figure 27). Thus, the range between the low and high exposure class is very small (18.6% to 19.4% of total population) and poverty is the main driving factor of potential severe health impacts.

## 7 Hazard projections: climate indices

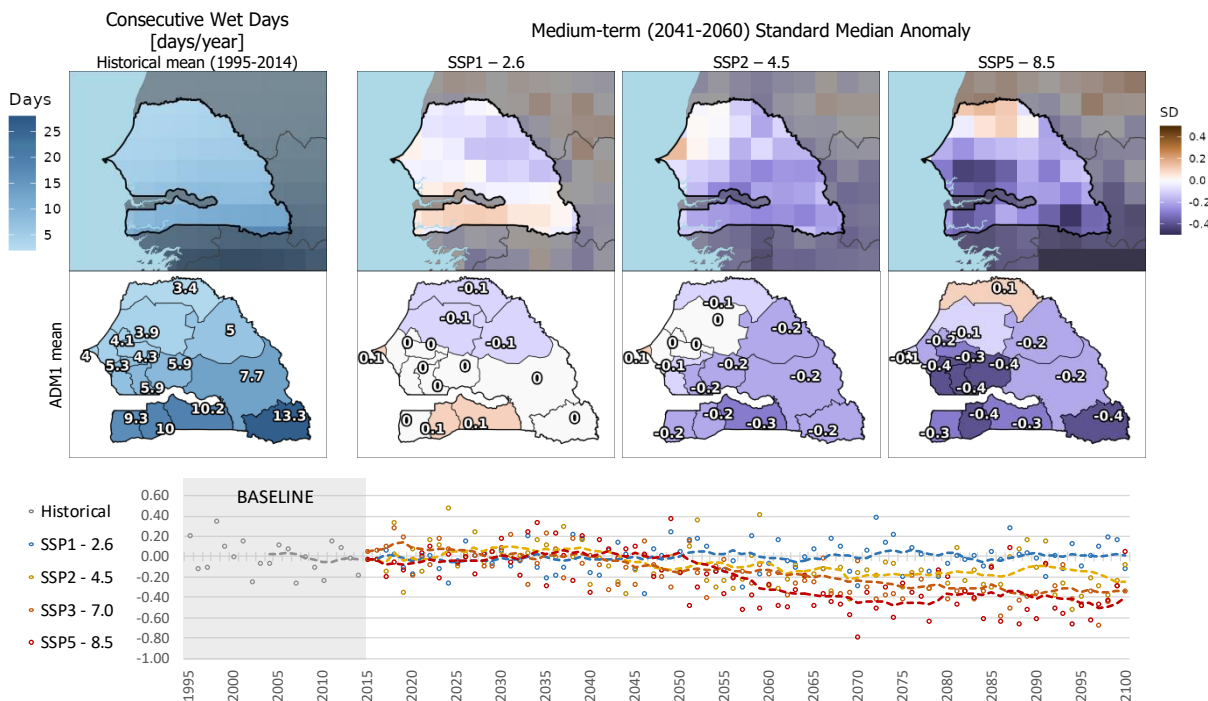
The climate indices associated with presented natural hazards are discussed below. Each of these mapping ensembles has a similar structure. The gridded historical mean over the baseline period 1995–2014 is shown in the top left, with the historical average over this period shown on the map at the bottom left. The second, third and fourth columns then represent the projected anomalies for the climate variables under SSP1 – 2.6 (second column), SSP2 – 4.5 (third column), and SSP5 – 8.5 (fourth column). The top row shows the gridded standardised anomalies derived from CMIP6 for our time horizon 2041–2060, while the bottom row shows the average standardised anomaly for each province in Senegal. Below the maps, for each climate variable, the historical variation during the baseline period is shown, together with the projected future anomalies for the three SSPs.

### 7.1 Rainfall indices

Four climate indices are assessed to estimate the change in extreme rainfall trends, which could ultimately affect flood and landslide hazards: annual number of consecutive wet days (CWD, *Figure 28*), annual days of rainfall with over 10mm of precipitation (R10mm, *Figure 29*), maximum precipitation over five days (Rx5day, *Figure 30*), precipitation amounts during extremely wet days (R99p, *Figure 31*), and the projected sea level rise (SLR, *Figure 32*).

The historical baseline for these indices shows increasing wet conditions from north to south, as previously described by the climatic classification. Looking at the future projections up to the end of the century the long term (timeseries), we notice that most changes are within the range of historical variability (SD between -1 and 1). Consecutive wet days are expected to slightly decrease toward the end of the timeseries, meaning that precipitation events could become shorter in the future. The change is more evident for higher emission scenarios (SSP3-7.0 and SSP5-8.5). The reduction is more significant in the central and southern region, while the northern region could see a slight increase.

*Figure 33: Climate indices – Consecutive Wet Days (days/year) for Senegal*



Looking at precipitation extremes, heavy precipitation days (rainfall > 10 mm) show fluctuations within a similar range for all emission scenarios, with a slight increase by the mid-century and a slight decrease afterward. Cumulated 5-days rainfall is expected to remain stable across all emission scenarios on the long term. However, extreme precipitation is expected to increase in most of the country, especially in wetter regions, and with larger intensity according to emissions. The intensity of change is rather small, but could translate into an increase of pluvial flood risk across urban areas, particularly because precipitation durations are expected to become shorter (see *Figure 33*), potentially leading to more intense and temporally concentrated precipitation events in the future.

*Figure 34: Climate indices – Rainfall over 10mm (days/year) for Senegal*

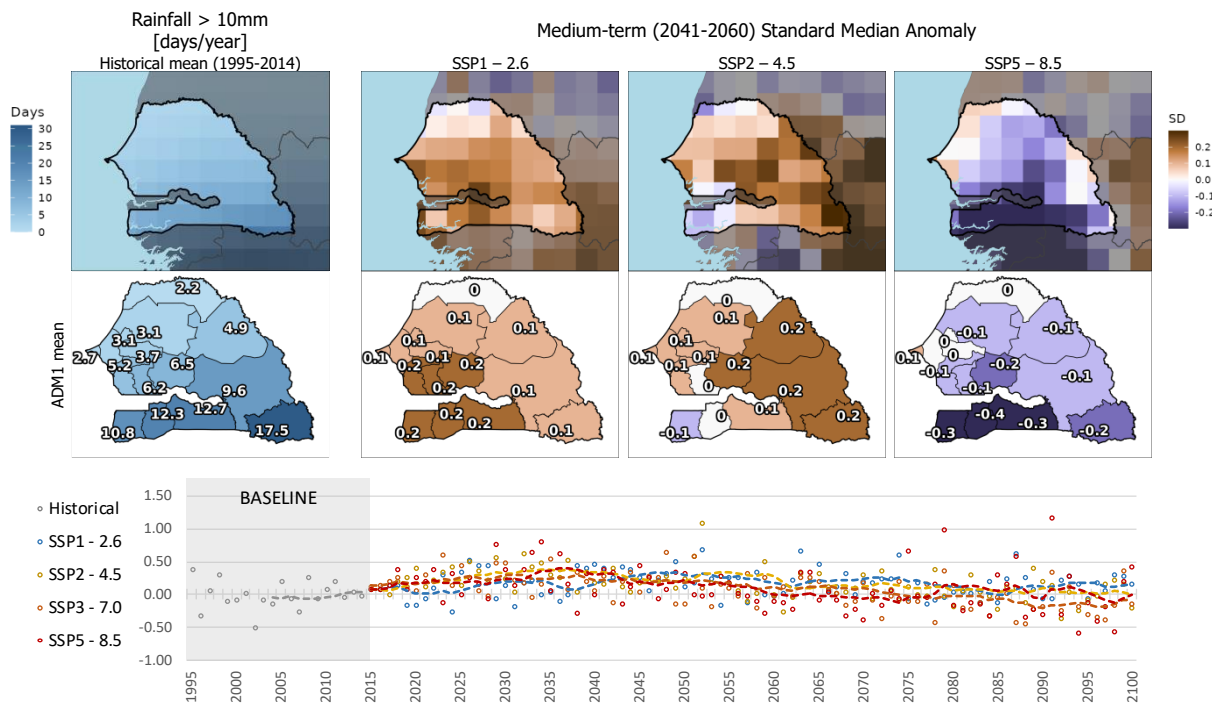


*Figure 35: Climate indices – Maximum 5-day Precipitation (mm/year) for Senegal*

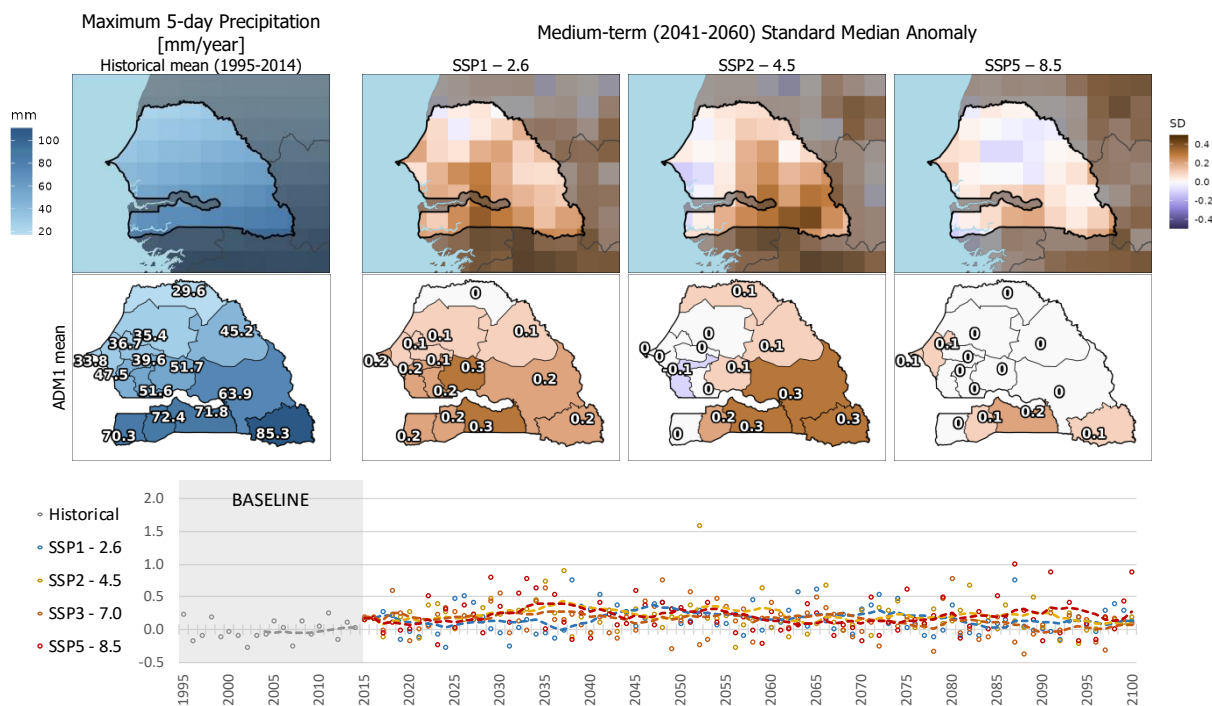
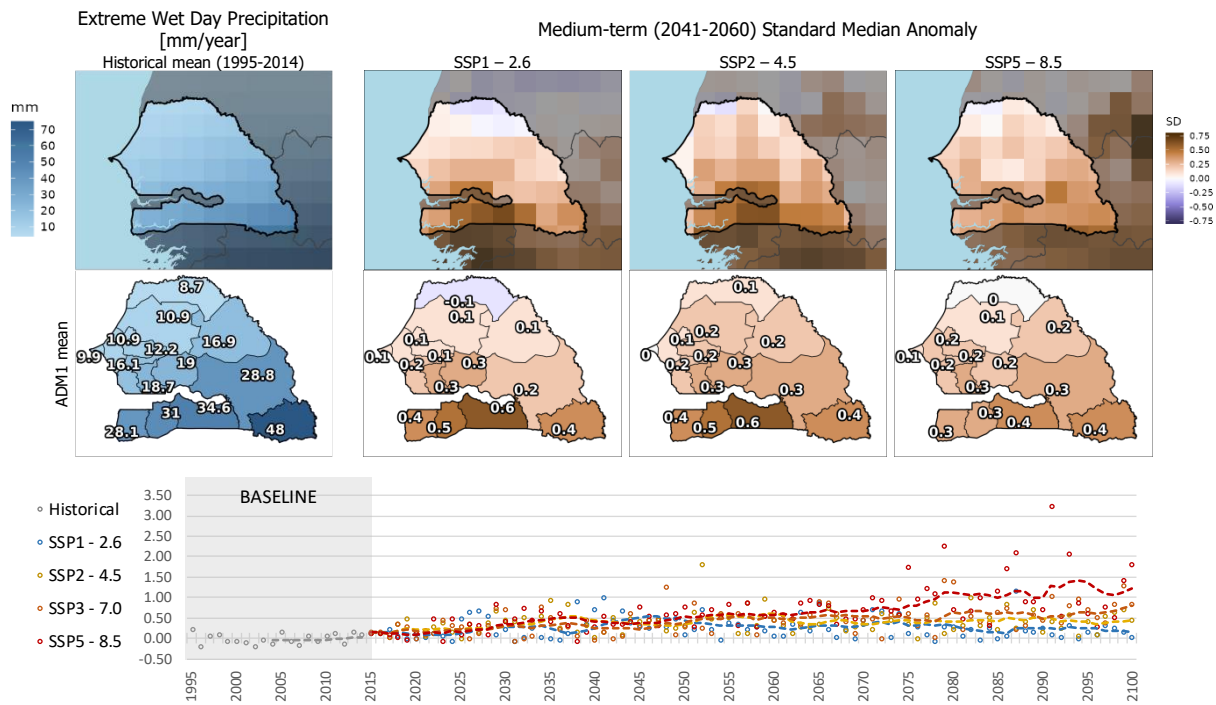
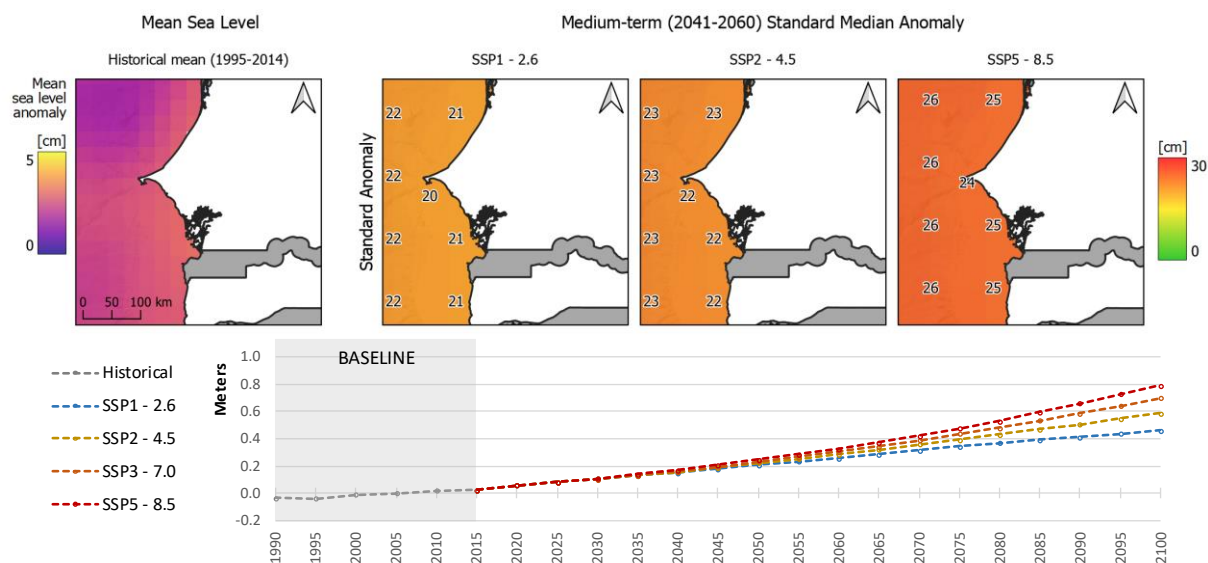


*Figure 36: Climate indices – Extreme Wet Day Precipitation (mm/year) for Senegal*



Along the coastlines of Senegal, sea level rise could become a reason of serious concerns, particularly for the low-lying city of Saint Louis. By mid-century, sea level rise of at least 20 cm is expected under all climate change scenarios. By the end of the century, however, sea level could rise by 40 cm to 80 cm for the scenarios SSP1-2.6 and SSP5-8.5, respectively.

*Figure 37: Climate indices – Average Sea Level Rise (cm) on Senegal coast*



## 7.2 Drought indices

Two variables underpin the projection of changes in drought patterns: the *number of consecutive dry days per year* (CDD, *Figure 34*), and the *12-month Standardized Precipitation-Evapotranspiration Index* (SPEI, *Figure 35*). The SPEI has been found to be closely related to drought impacts on ecosystems, crop, and water resources, and has been designed to take into account both precipitation and potential evapotranspiration in determining drought ([World Bank 2022](#)). Note that negative SPEI values indicate drier than normal conditions, while positive values indicate wetter than normal conditions. The mapping ensembles for these drought-related variables follow a similar design to the precipitation-related variables, again with the 1995-2014 period as a historical baseline.

The historical baseline shows that the north-western regions of Senegal experience more than 210 dry days annually, while the south-western region typically shows wetter conditions and shorter dry spells. This is not mirrored by the SPEI calculated over 12 months (annual mean), which measures water availability accounting for evapotranspiration; positive index values are found in the centre and north-east, while the west and the south-east show slightly negative values. The number of dry days is not expected to change drastically in the future, although all emission scenarios point towards a slight increase. The SPEI projected anomalies, on the other hand, suggest decreasing water availability in the north and north-east of the country, especially under high-emission scenarios. This could be explained by increasing temperatures that promote water evaporation. Overall, these two indices and the four precipitation indices suggest stable to slightly drier conditions for Senegal up to the end of the century, compared to the baseline.

*Figure 38: Climate indices – Consecutive Dry Days for Senegal*

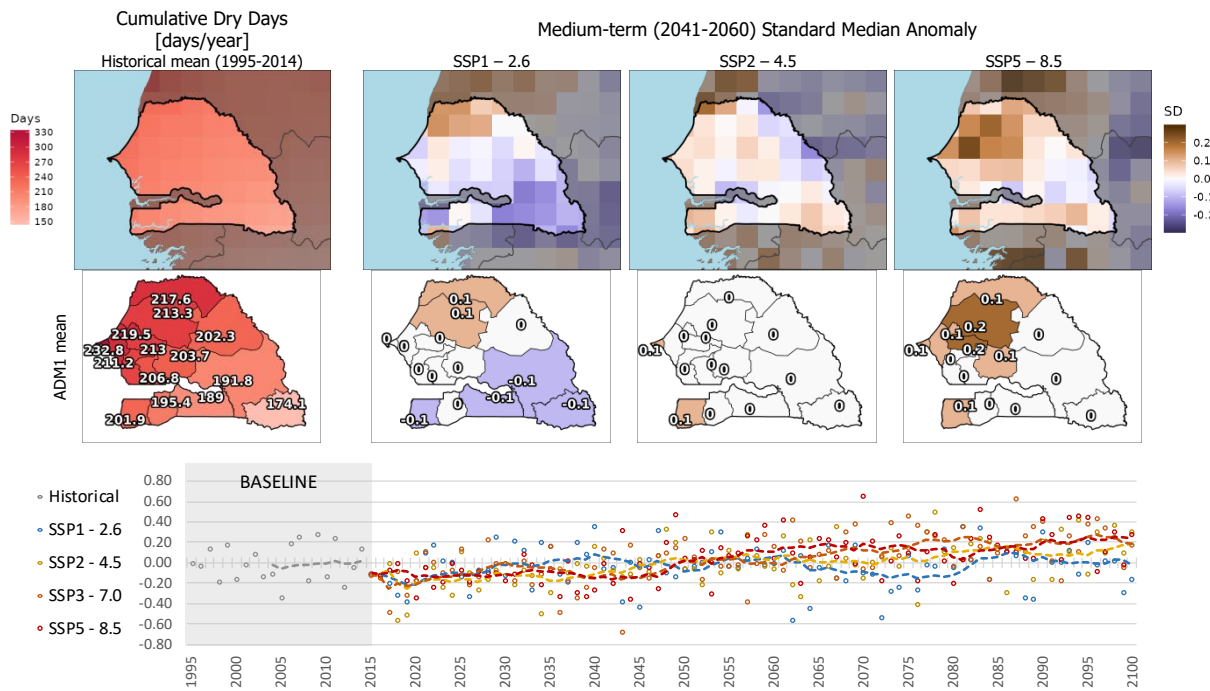
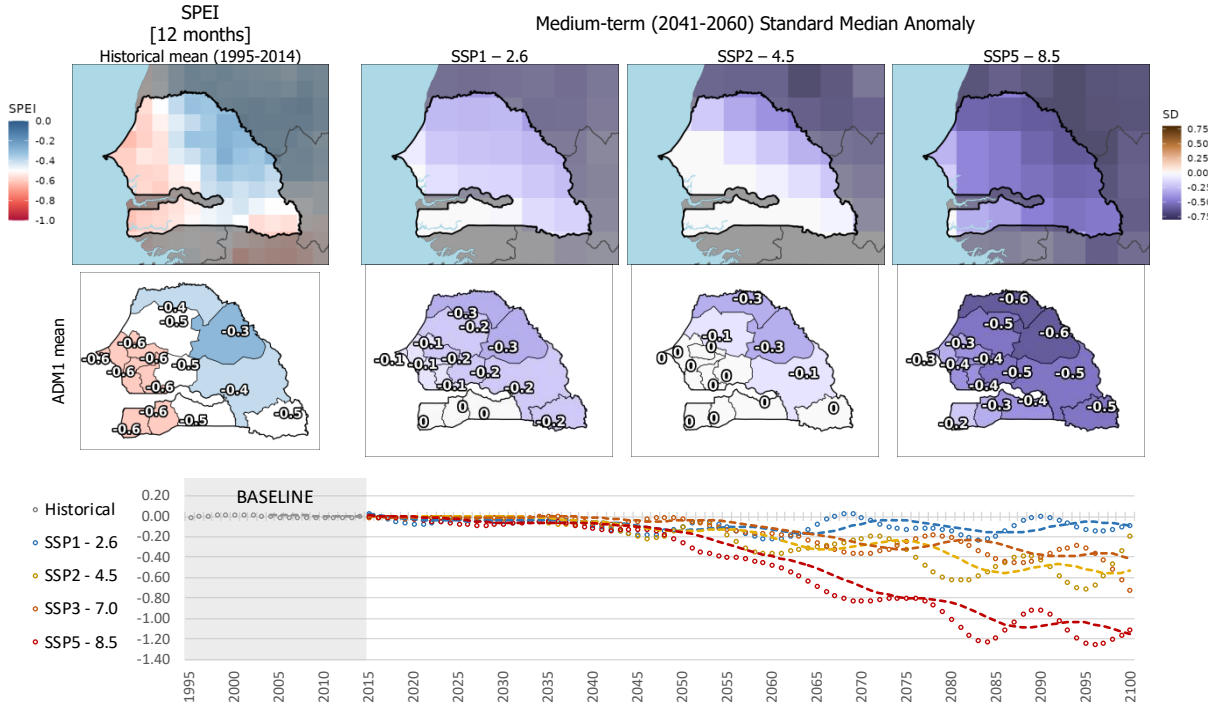


Figure 39: Climate indices – Standard Precipitation-Evapotranspiration Index for Senegal



### 7.3 Heat indices

The change in heat patterns under the three climate change scenarios is estimated by looking at the projections of the *WBGT heat index*. Changes in the frequency (i.e., number of days) of extreme heat events are analyzed. Of notable interest is the increased frequency in the occurrences of both the moderate (WBGT >23°C, Figure 36) and the extreme (WBGT >30°C, Figure 37) heat stress events in the region, which can potentially translate into unprecedented heat stress and mortality (even under the lower emission scenario). The long-term trend of the heat indices is particularly worrisome. Under SSP1, only a slight to moderate increase is expected in the total number of days over WBGT 23°C and 30°C with the chance to reduce the anomaly again by the end of the century; while both SSP2-4.5 and SSP5-8.5 project a steady and significant increase of hot days and especially extremely hot days, worsening the current risk picture for heat stress events.

The most vulnerable people to heat-related illnesses are workers who spend a substantial portion of the shift outdoors and those who work in hot and humid environment indoors: agricultural workers, miners, fishermen, construction/building workers, electricians, landscapers, ground maintenance, and factory workers [Bourbonnais et al., 2013; Lucas et al., 2014]. Considering that the agriculture sector employs the large majority of the active labor force and accounts for a large share of the gross domestic product, the projected heat stress threatening the workers' health can reduce productivity and undermine the region's economic development.

Under all three SSPs, the standardized anomalies of heat are forecasted to significantly increase relatively to the 1990-2010 reference base. This increase is considerably stronger under higher-emission future scenarios. Looking at days with a WBGT over 23 degrees (strong heat stress), the whole country is expected to get more frequent heat stress events as a consequence of a warmer climate, in particular extreme heat stress events could become much more frequent, especially in the innermost, flat regions. The number of warm nights is expected to increase uniformly in the country and proportionally to the intensity of the emission scenario. The projected rise in temperatures is

concerning, as it indicates increasing heat stress across Senegal, potentially putting even more lives at risk and raising awareness for the most vulnerable categories, such as children and the elderly.

*Figure 40: Climate indices – Days Wet-Bulb Globe Temperatures (WBGT °C) exceeding 23°C*

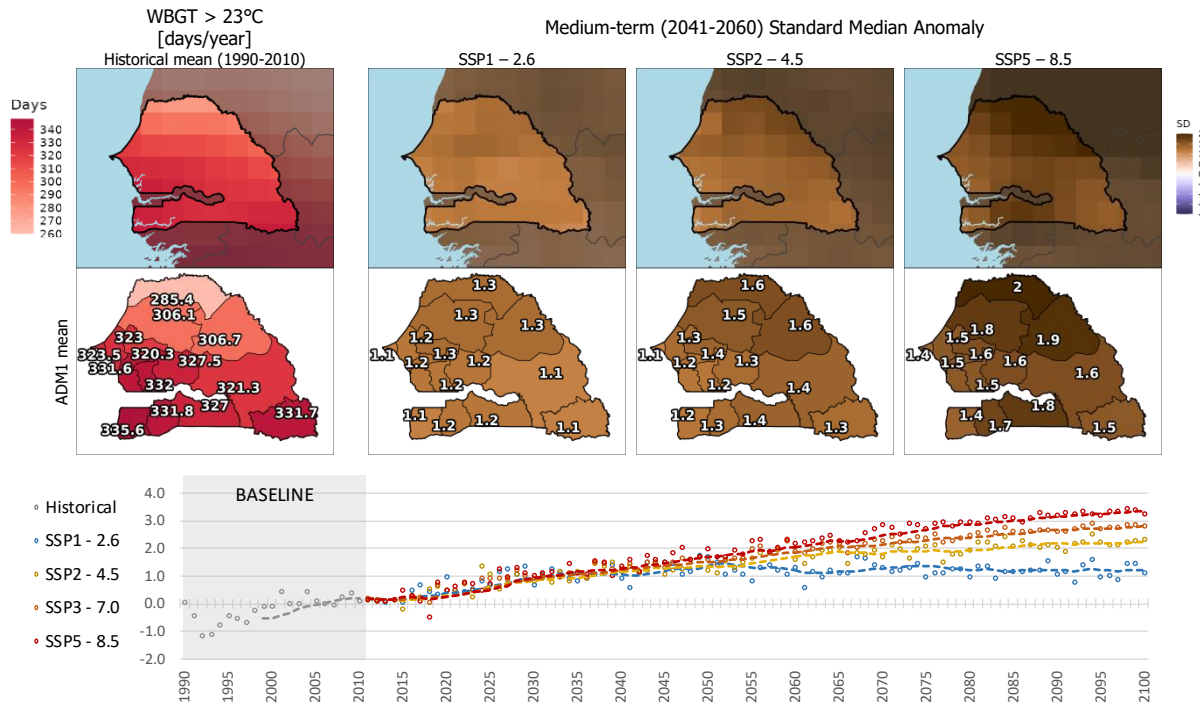
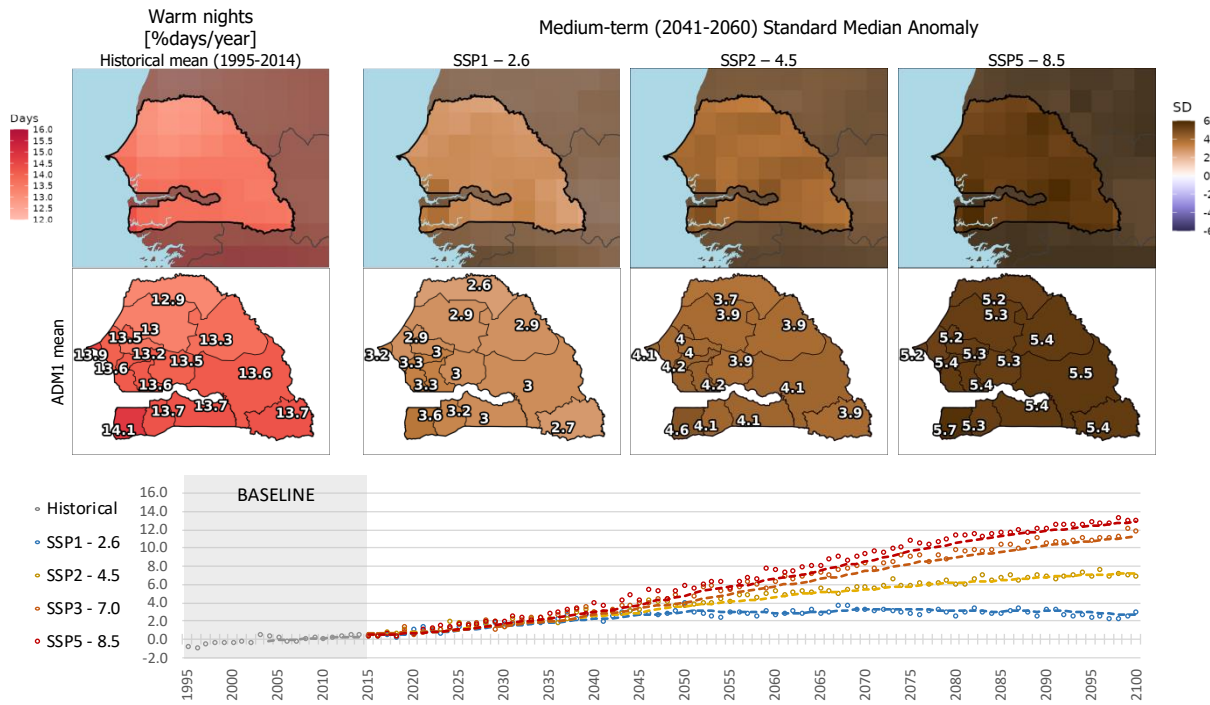


*Figure 41: Climate indices – Days with warm nights exceeding 30°C*



## 8 Annex 1 – Hazard models

### 8.1 Fluvial floods

<b>Name</b>	<a href="#">Fathom flood hazard maps v2</a>
<b>Developer</b>	Fathom
<b>Hazard process</b>	Fluvial flood
<b>Resolution</b>	90 m
<b>Analysis type</b>	Probabilistic
<b>Frequency type</b>	Return Period (10 RPs)
<b>Time reference</b>	Baseline (1989-2018)
<b>Intensity metric</b>	Water depth [m]
<b>License</b>	Commercial (acquired by World Bank)
<b>Notes</b>	“Undefended scenario” option is selected for the analysis.

### 8.2 Coastal floods / Storm surges

<b>Name</b>	<a href="#">Aqueduct flood hazard maps</a>
<b>Developer</b>	WRI - Deltares
<b>Hazard process</b>	Coastal flood
<b>Resolution</b>	1 km
<b>Analysis type</b>	Probabilistic
<b>Frequency type</b>	Return Period (10 RPs)
<b>Time reference</b>	Baseline (1960-1999)
<b>Intensity metric</b>	Water depth [m]
<b>License</b>	Open data
<b>Notes</b>	Includes effect of local subsidence.

### 8.3 Agricultural droughts

<b>Name</b>	<a href="#">Agricultural Stress Index (ASI)</a>
<b>Developer</b>	FAO
<b>Hazard process</b>	Agricultural drought
<b>Resolution</b>	1 km
<b>Analysis type</b>	Deterministic (remote sensing)
<b>Frequency type</b>	Occurrence frequency
<b>Time reference</b>	Baseline (1984-2020)
<b>Intensity metric</b>	Percentage of crop and pasture land affected by drought conditions across baseline period.
<b>License</b>	Open data
<b>Notes</b>	Aggregated from annual data scale.

## 8.4 Heat stress

<b>Name</b>	<a href="#">Global extreme temperatures (WBGT)</a>
<b>Developer</b>	VITO
<b>Hazard process</b>	Extreme heat
<b>Resolution</b>	10 km
<b>Analysis type</b>	Probabilistic
<b>Frequency type</b>	Return Period (3 RPs)
<b>Time reference</b>	Baseline (1981-2010)
<b>Intensity metric</b>	Wet Bulb Globe Temperature [°C]
<b>License</b>	Open data
<b>Notes</b>	Simplified wet bulb globe temperature defined as: $WBGT = 0.567 T + 0.393 VP + 3.94$ with T the air temperature (in °C) and VP the vapour pressure (in hPa) (WMO, 2015)

## 8.5 Tropical Cyclones

<b>Name</b>	<a href="#">STORM tropical cyclone wind speed</a>
<b>Developer</b>	STORM – Deltares
<b>Resolution</b>	10 km x 10 km
<b>Analysis type</b>	Probabilistic
<b>Frequency type</b>	Return Period (6 RPs)
<b>Time reference</b>	1980-2018
<b>Intensity metric</b>	Maximum wind speeds [m/s]
<b>License</b>	Open data
<b>Notes</b>	Data is available for every ocean basin. Return periods were empirically calculated using a Weibull's distribution.

<b>Name</b>	<a href="#">IBTrACS v4</a>
<b>Developer</b>	NOAA - NCEI
<b>Resolution</b>	Individual events
<b>Analysis type</b>	Observations
<b>Frequency type</b>	none
<b>Time reference</b>	1980-2022
<b>Intensity metric</b>	Category, wind speed
<b>License</b>	Open data

## 8.6 Air pollution

<b>Name</b>	<a href="#">ACAG surface PM2.5</a>
<b>Developer</b>	Van Donkelaar et al., Washington University
<b>Resolution</b>	1 km x 1 km
<b>Analysis type</b>	Deterministic
<b>Time reference</b>	1998-2020
<b>Intensity metric</b>	PM 2.5 concentration
<b>License</b>	Open data
<b>Notes</b>	Based on MODIS, MISR, SeaWiFS data. Aggregated from annual data scale.

## 9 Annex 2 – Exposure models

### 9.1 Population

<b>Name</b>	<a href="#">Global Human Settlement Layer</a>
<b>Source</b>	EU Joint Research Center
<b>Format</b>	Raster grid
<b>Resolution</b>	100 m
<b>Time reference</b>	2020
<b>Metric</b>	Population count
<b>License</b>	Open
<b>Notes</b>	Constrained to built-up (2020)

### 9.2 Built-up

<b>Name</b>	<a href="#">World Settlement Footprints</a>
<b>Developer</b>	ESA
<b>Format</b>	Raster grid
<b>Resolution</b>	10 m
<b>Time reference</b>	2019
<b>Metric</b>	Presence of built-up (binary)
<b>License</b>	Open

### 9.3 Land cover and land use

<b>Name</b>	<a href="#">ESA WorldCover</a>
<b>Developer</b>	VITO and consortium for ESA
<b>Format</b>	Raster
<b>Resolution</b>	10 m
<b>Time reference</b>	2020
<b>Metric</b>	Land cover classes
<b>License</b>	Open

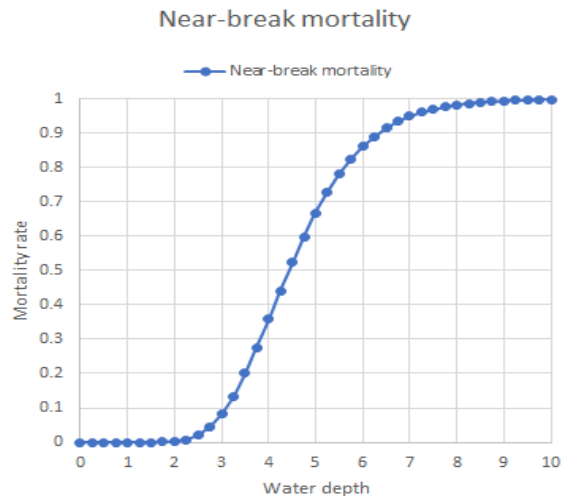
## 10 Annex 3 - Vulnerability functions, thresholds, and calculations

### 10.1 Floods (river and coastal)

**Population:** Generalized mortality function for people located close to dam break ([Jonkman et al. 2008](#))

Approximated by:

$$y = \frac{0.985}{1 + e^{(6.32 - 1.412x)}}$$

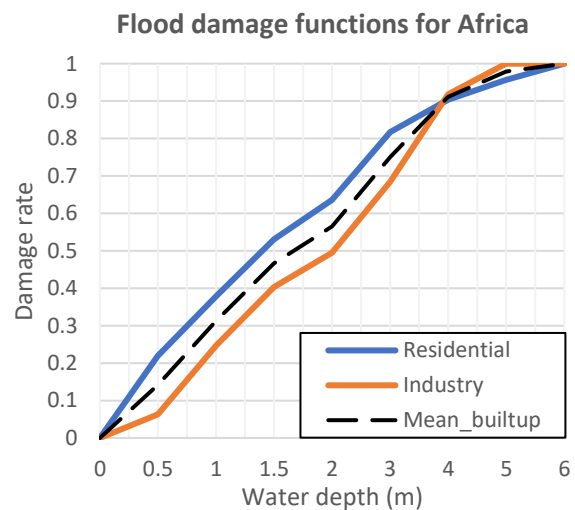


**Built-up:** regionalized (continent) impact function for land cover categories ([Huizinga et al. 2017](#))

- Mean function for built-up area classes, including residential and industrial categories

Approximated by:

$$y = 0.0095x + 0.0362(x^2) - 0.0028(x^3)$$



**Agriculture:** classification of exposure for water depth > 0.5 m

Class	Water depth range (m)
C1	0.01 - 0.15
C2	0.15 - 0.5
C3	0.5 - 1
C4	1 - 1.5
C5	1.5 - 2
C6	> 2

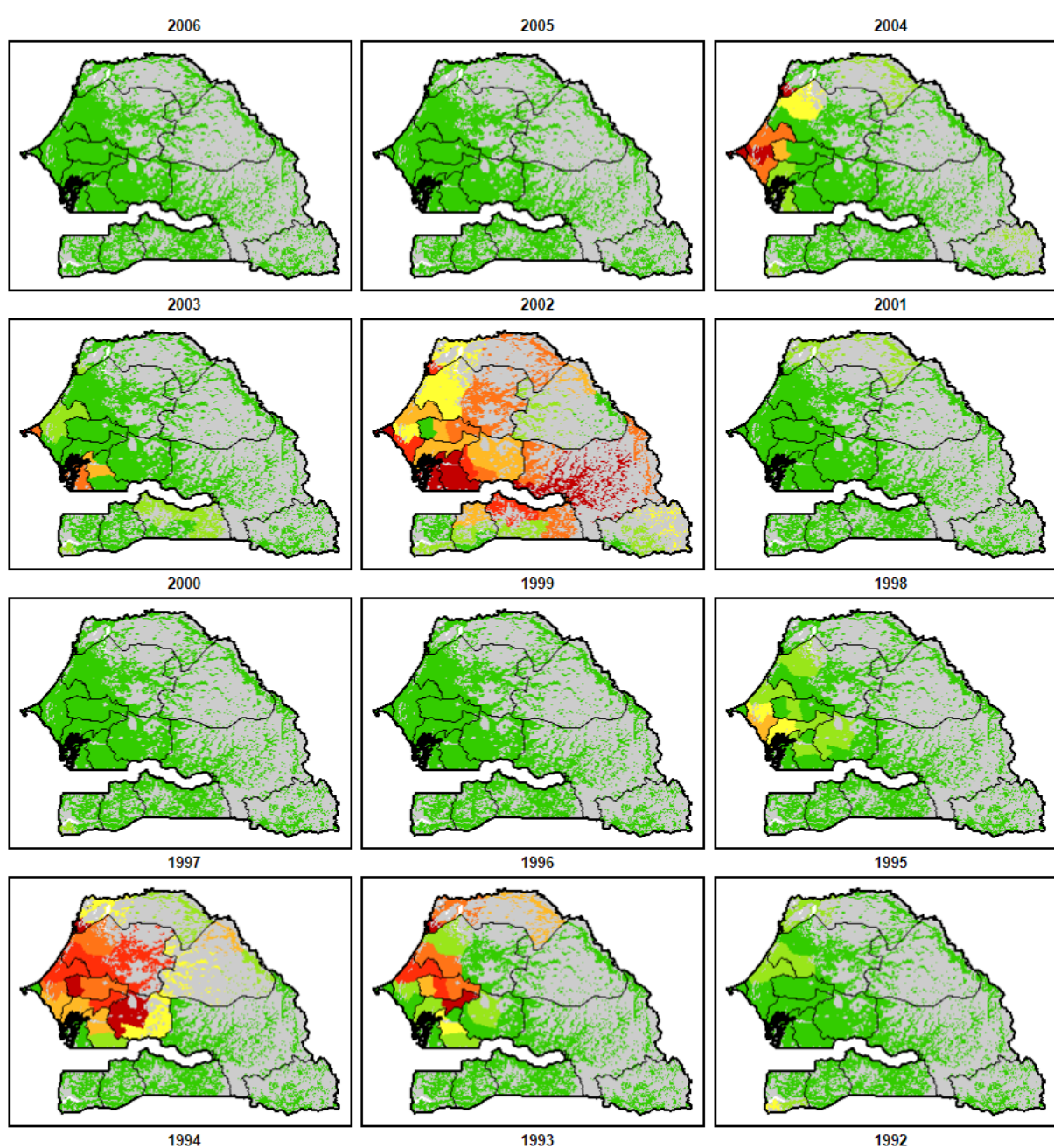
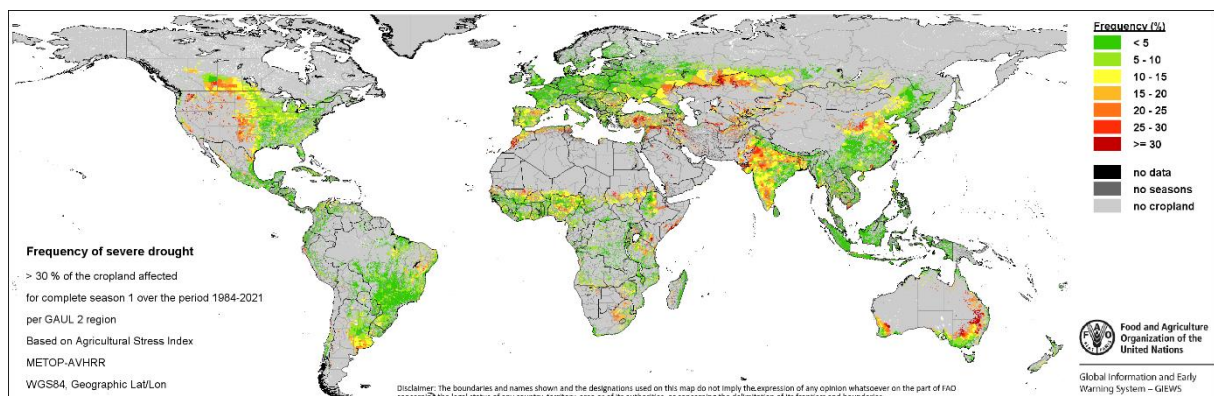
### 10.2 Landslides

**Built-up and Population:** ARUP index classification. “High hazard” class (C3) is plotted in maps; if empty, C2 (“medium hazard”) is plotted.

ARUP intensity index	Class
< 0.001	Low
0.001 – 0.01	Medium
> 0.01	High

### 10.3 Drought (water stress on agriculture)

**Agriculture:** [FAO ASIS](#) standard classification; frequency of impact over >30% or >50% of cropland.



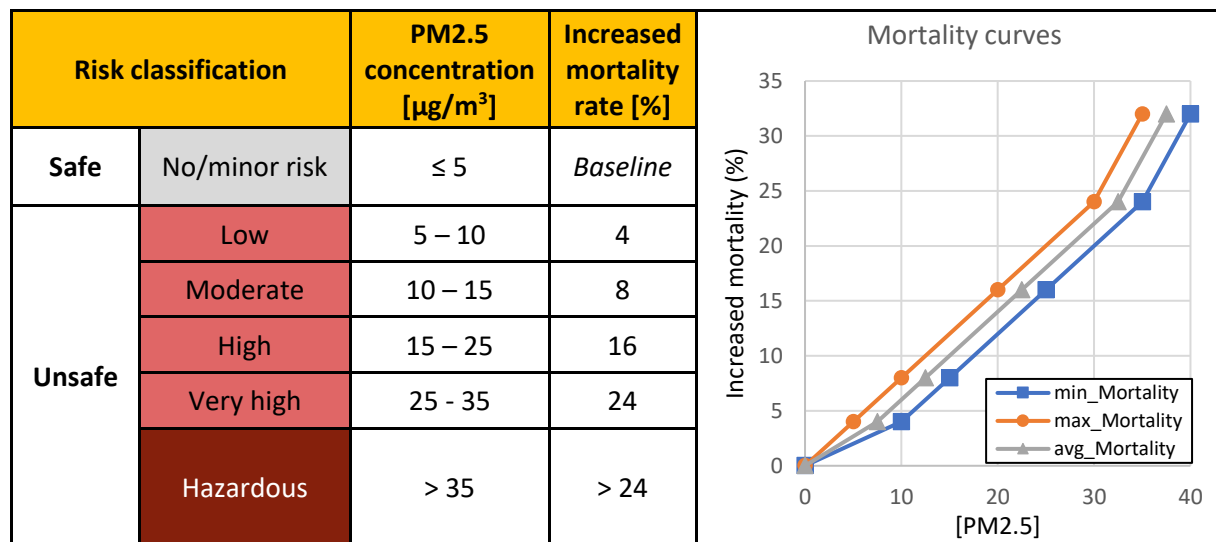
## 10.4 Heat stress

**Population:** standard heat stress classification ([Blazejczyk et al. 2012](#)) for Wet-Bulb Globe Temperature (°C).

WBGT (°C)	Stress category (population)
> 30	Extreme heat
28 to 30	Intense heat
23 to 28	Strong heat
18 to 23	Moderate heat
<18	No thermal stress

## 10.5 Air pollution

**Population:** mortality function in relation to PM2.5 concentration. Risk classes according to [WHO Air Quality guidelines \(2021\)](#).



## 10.6 Relative Wealth Index

Obtained from [HDX](#) for the year 2020. Point data are first rasterized at the original resolution (2.4 km), then weighted using GHS population layer at 100 m. Finally, it is summarized at ADM 3 level.

